Developing an ice strength algorithm for sub-Arctic regions

Johnston, M.; Timco, G.

Publisher's version / Version de l'éditeur:
https://doi.org/10.4224/12329076
Technical Report, 2004-03

Developing an Ice Strength Algorithm for Sub-Arctic Regions

M. Johnston and G. Timco

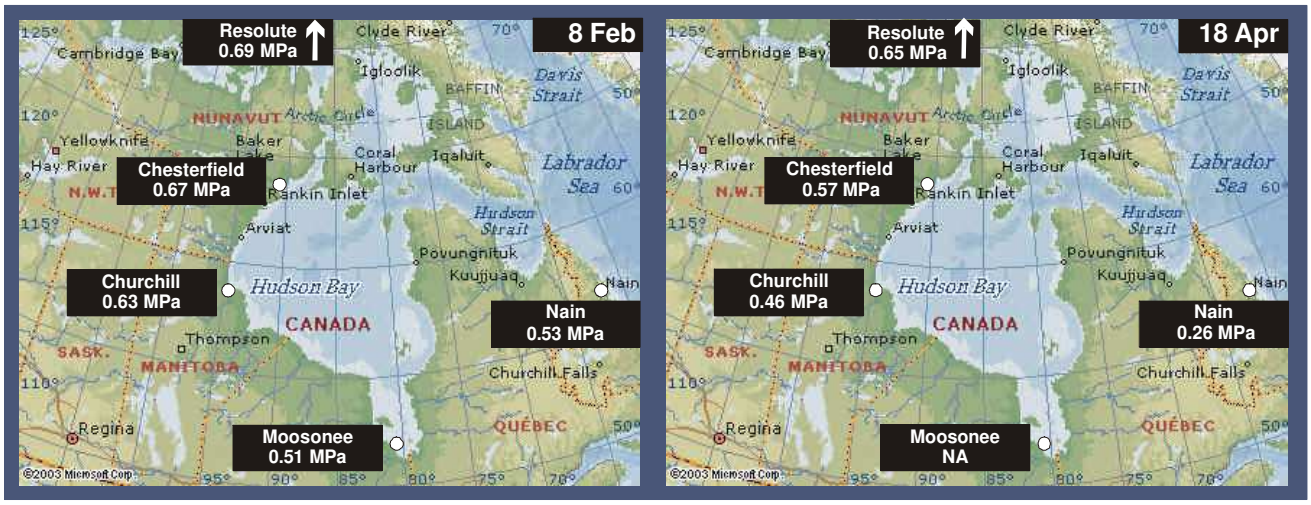

Technical Report, CHC-TR-023

March 2004

CHC CANADIAN HYDRAULICS CENTRE

Developing an Ice Strength Algorithm for Sub-Arctic Regions

M. Johnston and G. Timco
Canadian Hydraulics Centre
National Research Council of Canada
Montreal Road
Ottawa, Ontario K1A 0R6

Prepared for:
Canadian Ice Service
373 Sussex Drive, Bld. E-3
Ottawa, Ontario K1A 0H3

Technical Report, CHC-TR-023

March 2004

Abstract

This study, the first year of a two-year study, was undertaken to determine whether the algorithm that is used to describe the seasonal decrease in strength of landfast, first-year ice in the high Arctic can also be used for sub-Arctic first-year ice. The strength algorithm is the basis of the Ice Strength Charts issued by Canadian Ice Service. The method used to formulate an Ice Strength Algorithm for the high Arctic and its applicability for sub-Arctic ice are discussed. The report outlines the steps taken to develop the strength algorithm for sub-Arctic areas. Relevant data on the properties of sub-Arctic ice are compiled and an approach for including sub-Arctic regions in future Ice Strength Charts is suggested. Emphasis is given to level first-year ice along the Labrador coast and in Hudson Bay.

Table of Contents

List of Figures

List of Tables

Developing an Ice Strength Algorithm for Sub-Arctic Regions

1.0 Introduction

From 2000 to 2002, the Canadian Hydraulics Centre (CHC) conducted measurements on first-year ice in the high Arctic to document changes occurring in the ice from spring to summer. Field measurements included snow and ice thickness, ice temperature and salinity and the *in situ* ice borehole strength. Data acquired during those three years were used to formulate an equation, or strength algorithm, that was used as the basis for prototype Ice Strength Charts. The Ice Strength Charts have been issued by Canadian Ice Service (CIS) from May to August. To date, they have been issued only for landfast, level first-year ice in the high Arctic. This study was undertaken to assess the possibility of using the same algorithm, or developing a new one, to describe the strength of ice south of the Arctic, in the so-called sub-Arctic.

The cursory examination conducted by Johnston and Timco (2003-a) showed that the strength algorithm for first-year ice in the high Arctic should not be extended to the same ice type in sub-Arctic areas. Developing an algorithm for ice south of 60°N would require the following:

- itemize steps needed to develop a strength algorithm for sub-Arctic areas
- literature search to compile previously-measured properties of sub-Arctic ice
- develop an approach for including sub-Arctic regions in future Ice Strength Charts

This report, the first of a two-year study, provides an overview of the work done on the above-mentioned tasks. The mandate given to CHC by CIS indicated that emphasis should be given to level first-year ice along the Labrador coast and in Hudson Bay. During the second year of this project the proposed approach for including sub-Arctic ice in future Ice Strength Charts will be examined using temperature, salinity and strength measurements recently acquired on landfast, level first-year ice near Nain, Labrador. The Labrador field study is a two-year project that was sponsored jointly by Transport Canada and Canadian Ice Service. It will provide much needed data on the properties of sub-Arctic ice and their changes throughout spring and summer.

2.0 Outline of the Report

A number of steps were taken to develop an approach for including sub-Arctic ice in future Ice Strength Charts. This report documents those steps, which included:

- obtaining data to calculate the flexural strength of first-year ice
- examining air temperatures and ice thicknesses at five sites on Labrador Coast and in Hudson Bay
- calculating the seasonal decrease in flexural strength at those selected sites using mean daily air temperatures and estimated ice thickness
- calculating the flexural strength using existing ice property measurements and comparing them to calculations based on air temperatures and ice thickness
- examining the feasibility of relating the flexural strength of ice to accumulated degree days (ADD) at different latitudes
- basing future Ice Strength Charts on flexural strengths calculated directly from established equations
- using strength maps to visualize the decrease in strength of Arctic and sub-Arctic ice
- conclusions and recommendations
- literature review – list of abstracts

3.0 Approaches for Calculating the Flexural Strength of Ice

Several researchers have attempted to relate the strength of sea ice to the brine volume or total porosity of the ice. There is a good reason for this. It is generally assumed that as the total porosity in the ice increases, the strength should decrease. That is because there is less "solid ice" that has to be broken. Timco and O'Brien (1994) conducted the most comprehensive analysis of the flexural strength of ice. Their analysis was based upon approximately 1000 tests on sea ice and used over 2500 reported measurements on the flexural strength of freshwater ice and sea ice. The authors showed that the data for first-year sea ice could be described by the following equation:

$$\sigma_f = 1.76 \exp\left(-5.88 * \sqrt{\upsilon_b}\right) \qquad (1)$$

where σ_f is the flexural strength of the ice and the brine volume (ν_b) is expressed as a brine volume fraction. This relationship is shown with the data in Figure 2.

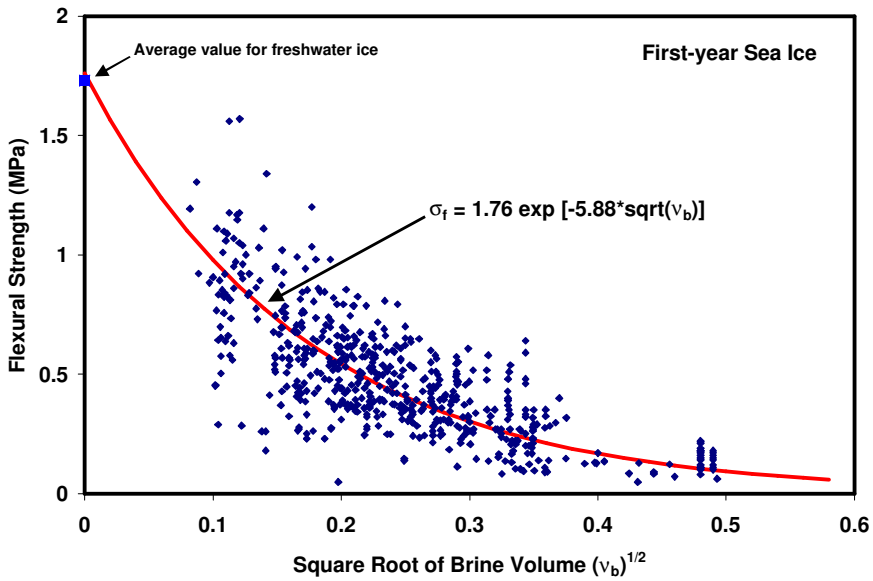

Figure 1 Flexural strength versus the square root of the brine volume for first-year sea ice

There are several points to note from Figure 1:

- The value of 1.76 MPa for zero brine volume is in excellent agreement with the average strength (1.73 MPa) measured for freshwater ice.
- The general scatter in the data increases with decreasing brine volume. This is a reflection of the fact that, at low brine volumes, the ice shows brittle behavior. The range of scatter approaches that measured for freshwater ice and is characteristic of a brittle material.
- This equation is the most comprehensive equation for flexural strength to date. There have been a few other equations proposed to relate strength and brine volume however those were based on substantially fewer data points and data that extended over a very limited range. In other words, the other equations are valid over only a small brine volume range. The wider range of this equation represents these other equations very well in the ranges in which they are valid.
- Data for the equation were compiled from a large number of investigators and from a variety of geographic locations in both polar and temperate climates. Therefore it should be quite representative of the flexural strength of sea ice in most regions.
- The brine volume used to represent the ice beam for any test was taken as the average brine volume, determined from the average ice temperature and salinity of the beam. Calculations of the flexural strength require the depth-averaged temperature of the ice (or bulk temperature) and depth-averaged salinity of the ice (bulk ice salinity).

3.1 Intrinsic versus Extrinsic Method of Calculating Flexural Strengths

The so-called intrinsic method can be used to calculate the flexural strength of the ice using measured, depth profiles of the ice temperature and ice salinity (which are intrinsic ice properties). If those ice property measurements are not available, an extrinsic method can be used to calculate the flexural strength of the ice. The extrinsic method uses the air temperature and ice thickness to estimate the depth-averaged (bulk) ice temperature and bulk ice salinity (Timco and Frederking, 1990).

Figure 2 shows the comparison between the flexural strengths calculated using the two different techniques. In case (a) the flexural strength was calculated by the intrinsic method, using the ice temperature and ice salinity (T_ice and S_ice) measured on first-year ice in the high Arctic in 2000 and 2001. In case (b), the flexural strength was calculated from the air temperature and ice thickness (T_air and h_ice) recorded in the high Arctic during the same period. The figure shows that the extrinsic method usually results in lower strengths than the intrinsic method, although the strengths on Julian Day (JD) 142 and JD149 were higher. It should be noted that the intrinsic method is preferred for calculating the flexural strength of the ice, however measuring ice properties can be both difficult and costly.

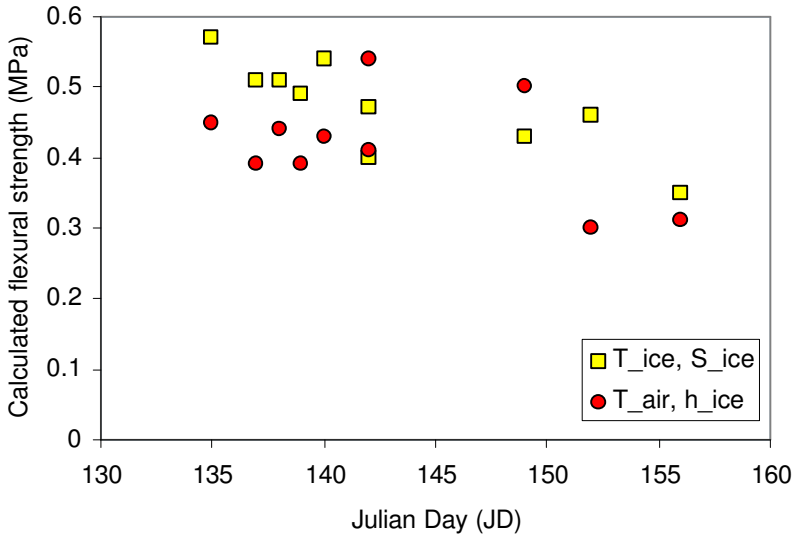

Figure 2 Comparison of two techniques for calculating flexural strength intrinsic method (T_ice and S_ice) vs. extrinsic method (T_air and h_ice)

4.0 Air temperature and Ice Thickness at Selected Sites

Since few property measurements have been made on ice along the Labrador Coast and virtually no measurements have been made on the ice in Hudson Bay (see literature review in Appendix A), it was necessary to use the extrinsic method for calculating the flexural strength of ice at different latitudes. As a result, Canadian Ice Service supplied CHC with air temperature and ice thickness data for nine climate stations in the area of interest, as shown in Figure 3.

Figure 3 Sites for which air temperature and ice thickness data were supplied

Although air temperature and ice thickness data were provided for nine sites, CIS suggested that efforts be focused upon ice along the Labrador coast and the western regions of Hudson Bay, since that is where shipping is most extensive. Therefore, only five of the sites in Figure 3 were included in this analysis: Nain, Moosonee, Churchill, Chesterfield and Resolute, each of which is labeled on a darkened background in Figure 3. Resolute was included in this analysis, for comparative purposes only, because its three years of property measurements had been used to derive an ice strength algorithm for the high Arctic (Johnston and Timco, 2003-a).

4.1 Air Temperatures at Selected Sites

Air temperatures were supplied for each of the sites shown in Figure 3. The supplied data represented two-week averages of the 30-year normal mean daily air temperatures (designated as the 'smoothed' 30-yr MDT). For purposes of continuity between the two consecutive years, the figure shows Julian Days (JD) extending beyond JD365.

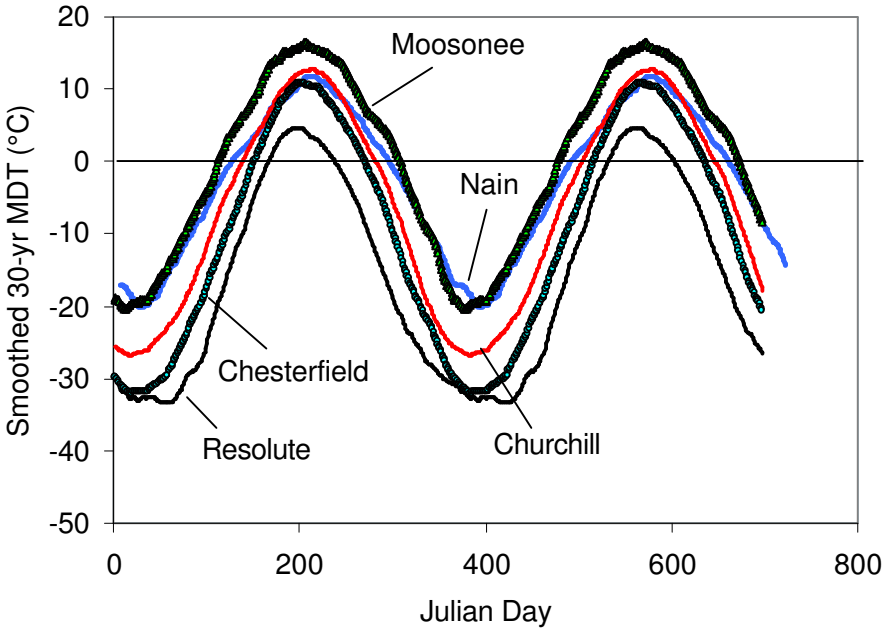

Figure 4 Two-week, smoothed 30-yr MDT for sites

Table 1 lists the minimum and maximum smoothed 30-yr MDT for each site and the dates on which they occur, along with the length of summer at the different sites. Summer was defined by the number of days that the smoothed 30-yr MDT remained above 0°C. Moosonee, the most southerly site, has the longest summer (196 days) and Resolute the shortest (72 days). Minimum temperatures at Nain and Moosonee are similar in winter (-20°C), however Moosonee experiences its coldest temperature about one week before Nain. In summer, temperatures in Nain are more like Churchill, with a maximum temperature of about +12°C that occurs on 30 July (JD576). In comparison, the maximum, smoothed 30-yr MDT at Moosonee is +16.5°C in summer and occurs on 26 July (JD572). Minimum averaged MDT at Resolute and Chesterfield are similar (-32°C and -33°C) although the coldest temperature in Resolute occurs about one month later than Chesterfield. As a result, the two sites have different lengths of winter. The summer maximum 30-yr MDT at Resolute and Chesterfield occur about the same time (16 July, JD562), yet differ by several degrees (+4.6°C in Resolute and +10.9°C in Chesterfield).

Table 1 Climate at Each of the Selected Sites, based on smoothed 30-yr MDT

Site	Min temp (°C)/ Date	Max temp (°C)/ Date	Summer (days)	Summer season
Moosonee	-20.3°C/ 13 Jan (JD378)	+16.5°C / 26 Jul (JD572)	196	23 Apr-5 Nov (JD113-309)
Nain	-20.2°C / 28 Jan (JD393)	+11.9°C / 30 Jul (JD576)	170	7 May -24 Oct (JD127-297)
Churchill	-26.9°C / 18 Jan (JD383)	+12.7°C / 31 Jul (JD567)	142	20 May-9 Oct (JD140-282)
Chesterfield	-32.0°C / 18 Jan (JD383)	+10.9°C / 21 Jul (JD567)	120	1 Jun-29 Sep (JD152-272)
Resolute	-33.4°C / 24 Feb (JD420)	+4.6°C / 16 Jul (JD562)	72	16 Jun-27 Aug (JD167-239)

4.2 Ice Thickness at Selected Sites

Canadian Ice Service provided CHC with digital information on the mean ice thickness for the five selected sites shown in Figure 3. The ice thickness data were compared to the ice thicknesses measured each year at the selected sites (Bilello, 1960, 1980; Bilello and Bates, 1991) and those from the CIS website (http://ice-glaces.ec.gc.ca).

Table 2 lists the years over which data were collected at each of the sites and the total number of data points for each site. In general, ice thickness measurements were made several times each week at the different sites. Since ice thickness information was not available for Nain, data were included for Hopedale, a coastal community 150 km south of Nain.

Table 2 Duration of Historical Data on Ice Thickness Measurements

Site	Measurement years	Data points
Moosonee	1959 - 1993	628
Hopedale	1960 - 1984	336
Churchill	1960 - 1987	465
Chesterfield	1959 - 1981	612
Resolute	1947 - 2003	1645

Figure 5 shows ice thickness data for the southern most (Moosonee) and northernmost (Resolute) sites. The figure shows historical ice thicknesses (circular data markers), a polynomial fit through the historical thickness data (solid line) and mean ice thickness data provided by CIS (yellow triangular data markers). Comparison shows that although there is a wide range of scatter in ice thickness measurements over the years, the CIS data agree favorably with the polynomial curve (solid line). The polynomials for calculating the seasonal increase and decrease in ice thickness for the five sites are included in Appendix B, expressed as a function of the continuous, two-year Julian Day. Appendix B also contains plots of measured and calculated ice thicknesses for all five sites.

Figure 6 compares results from the five polynomials that describe the increase and decrease in ice thickness at each site. The ice thickness at Hopedale and Moosonee are comparable. That is not surprising, considering air temperatures at the two sites were also similar during winter. What is surprising, however, is that the mean ice thicknesses at Churchill, Chesterfield and Resolute are all in good agreement. Recall that the mid-winter minimum 30-yr MDT for Churchill was about 10°C warmer than either Chesterfield or Resolute (about -32°C, Figure 4). Bilello (1980) states that the Churchill ice thickness measurements were frequently made near the mouth of the Churchill River, where the ice would have been thicker than typical first-year sea ice in that region. Other measurements were made in Churchill Harbour (Bilello and Bates, 1991; Bilello and Lunardini, 1996). The anomaly should be kept in mind when comparing the ice at Churchill to the other sites.

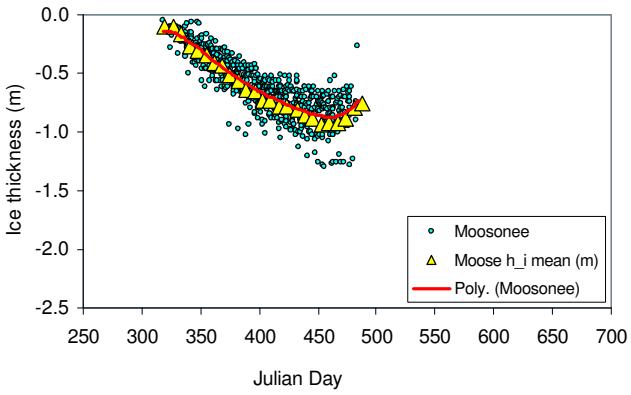

(a) Moosonee

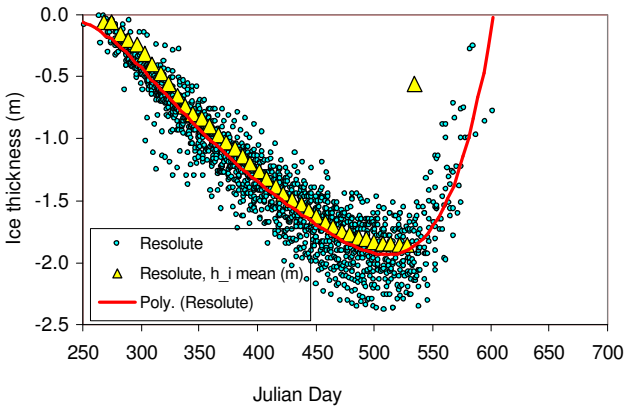

(b) Resolute

Figure 5 Ice thickness data for Moosonee and Resolute
(see Appendix B for additional sites)

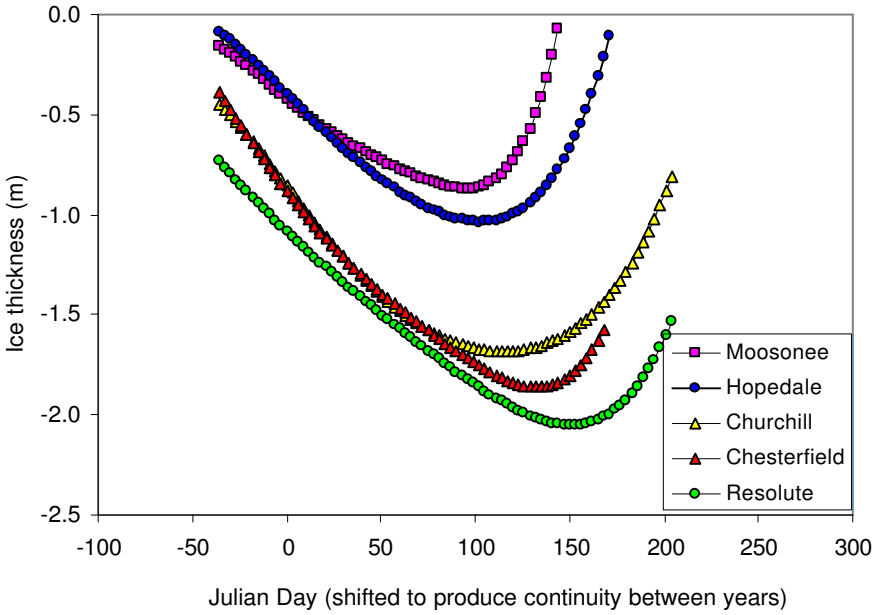

Figure 6 Comparison of ice thickness obtained from polynomial expression

5.0 Flexural Strength of sub-Arctic Ice using MDT and Ice Thickness

Figure 7 shows the flexural strengths calculated using the smoothed 30-yr MDT and mean ice thickness data[1] for each site. The figure makes four points immediately apparent: 1) as expected, the maximum flexural strength differs for each site, 2) the initial decrease in ice strength at each site occurs at different times, 3) the decrease in strength follows a similar trend for each site and 4) the strength begins to decrease well before the ice begins to ablate.

5.1 Peak Flexural Strength of Ice at Different Latitudes

Table 3 lists the peak, calculated flexural strengths for each site and shows the date on which they occur. Peak flexural strengths for the five selected sites ranged from 0.52 to 0.71 MPa and showed a systematic decrease with decreasing latitude (Figure 7). The sites fall into two groups, each with similar ice thicknesses and flexural strengths. The first group consists of Moosonee and Nain and the second group includes Churchill, Chesterfield and Resolute. The anomalously thick ice at Churchill resulted in flexural strengths that were 0.10 MPa greater than the ice strength determined for Nain or Moosonee. Flexural strengths for the Churchill site should be reassessed should more accurate ice thickness measurements come available.

[1] Ice thickness was determined from the polynomials listed in Appendix B

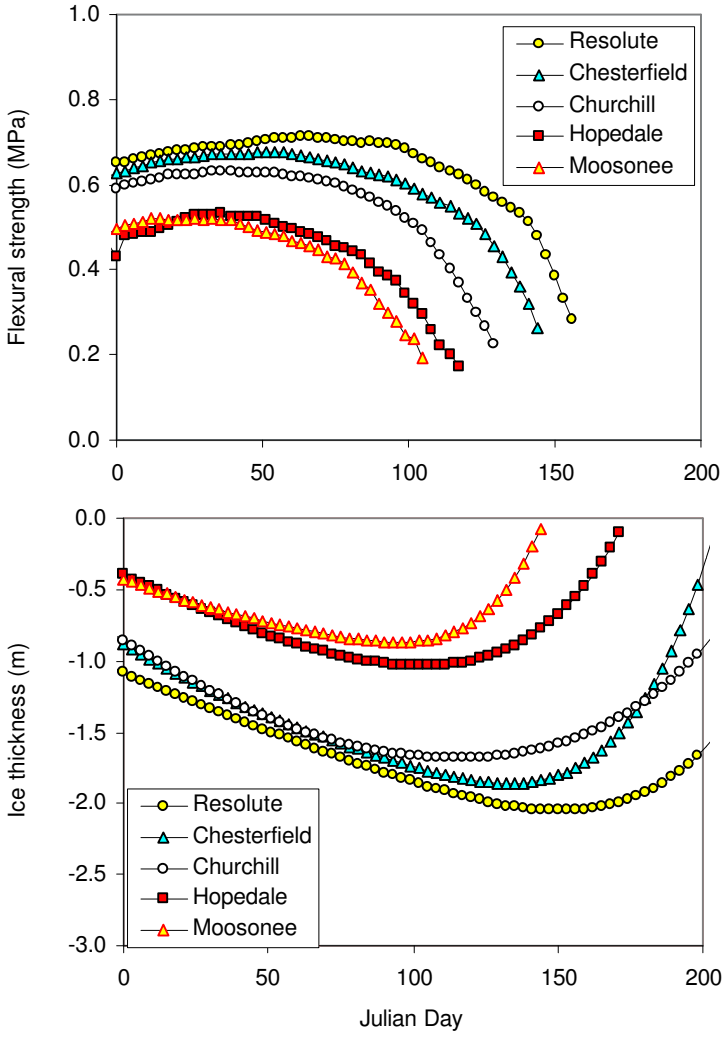

Figure 7 Seasonal decrease in flexural strength and ice thickness at different sites

Figure 7 shows that level first-year ice at Moosonee had the lowest calculated flexural strength. The maximum for that site was 0.52 MPa and occurred on January 12 (JD12). In comparison, the peak, calculated flexural strength at Resolute was 0.71 MPa and occurred on February 23 (JD54). The ice strengths at the different sites and their seasonal trends are significant because they show that the warmer temperatures in sub-Arctic areas result in a shorter ice growth season, which prevents the ice from developing a strength comparable to Arctic ice. For the most part, sub-Arctic ice has a peak flexural strength that occurs earlier and begins to decrease sooner than ice in the Arctic, as discussed subsequently.

Table 3 Calculated Flexural Strengths for Selected Sites

Site	Max flexural strength (MPa) / Date	Date of initial decrease in strength	Last calculated strength (MPa) / Date
Moosonee	0.52 / Jan 12 (JD12)	Feb 8 (JD39)	0.19 / Apr 14 (JD105)
Hopedale/Nain	0.53 / Jan 27 (JD27)	Feb 11 (JD42)	0.17 / Apr 26 (JD117)
Churchill	0.63 / Jan 30 (JD30)	Feb 26 (JD57)	0.23 / May 8 (JD129)
Chesterfield	0.67 / Jan 27 (JD27)	Mar 6 (JD66)	0.26 / May 23 (JD144)
Resolute	0.71 / Feb 23 (JD54)	Mar 18 (JD78)	0.28 / Jun 4 (JD156)

5.2 Initial Seasonal Decrease in Flexural Strength

Because the sub-Arctic has a shorter ice growth season, its first-year ice is thinner and begins to decrease in strength earlier than first-year ice in the Arctic. Based upon the calculations, the strength of first-year ice near Moosonee begins to decrease around February 8 (JD39). Ice near Nain begins to lose strength three days later, on February 11 (JD42). At Churchill, Chesterfield and Resolute, the ice strength begins to decrease on February 26, March 6 and March 18 respectively.

The data compiled by Timco and O'Brien (1994) do not support using the relation between flexural strength and brine volume beyond a square root of brine volume fraction of 0.5. Above that value, excessive brine volume causes inaccuracies in the flexural strengths measured from prepared samples -- measurements upon which the equation is based. Table 3 lists the dates to which the calculated flexural strengths are valid and the strength corresponding to that date. Based upon the smoothed 30-yr MDT and mean ice thickness, the technique developed by Timco and O'Brien (1994) can be used to calculate the flexural strength of ice near Moosonee and Nain until mid to late-April, by which time the strength is near 0.18 MPa (compared to a maximum of 0.52 MPa). The flexural strength at Churchill can be calculated until about the first week of May whereas it can be calculated until late May and early June at Chesterfield and Resolute, respectively. Had ice property measurements been available for those sites, the flexural strengths could have been calculated about one month later (Johnston and Timco, 2003-a).

5.3 Relation between Decrease in Ice Strength and Ice Ablation

Realizing the limitations of the flexural strength equation, the borehole jack system was used to measure the seasonal decrease of strength in Arctic first-year ice from 2000 to 2002. The borehole jack is extremely valuable because it provides a measure of the *in situ* ice strength, which does not require sample preparation. In regions where data overlap, the borehole strength of Arctic ice showed the same type of seasonal decrease in strength observed in the calculated flexural strengths (Johnston et al., 2002).

The borehole jack tests showed that the decrease in ice strength precedes the onset of ice ablation by more than one month (Johnston et al., 2003-b). That same trend is seen in the calculated flexural strengths (Figure 7). Results have shown that decrease in strength is related to increases in the ice temperature. *In situ* ice temperature measurements made from winter to spring at Canada Point, Navy Board Inlet (Frederking, personal communication) showed that Arctic first-year ice begins to warm throughout its full thickness around March 12, which is well before the ice typically begins to thin (Johnston and Timco, 2003-a). *In situ* ice temperature measurements similar to those conducted at Canada Point are currently being made in first-year ice off the Labrador coast. Those data will provide information about the seasonal temperature changes that occur in sub-Arctic ice.

6.0 Flexural Strength of sub-Arctic Ice using Property Measurements

Appendix A lists the references and abstracts that were compiled when searching for data on the ice conditions around Labrador and Hudson Bay. The literature search showed that few ice property measurements have been conducted off the Labrador coast and even fewer in Hudson Bay. The following is a summary of the highest quality data that were obtained on landfast first-year ice off the Labrador coast.

Gow (1987) – ice thickness and ice salinity were measured on first-year ice in Hebron Fjord in late May from the *POLARSTERN*. Although air temperatures and ice temperatures were not provided, the author stated that the ice had reached an isothermal state by late May.

Weeks and Lee (1958) – air temperature, ice thickness and ice salinity were measured in level first-year ice near Hopedale on March 16, April 4 and May 3. A bulk ice temperature was calculated using the air temperature and ice thickness, for the purpose of this study.

Cormorant Ltd. (1997) – depth profiles of the ice salinity and ice temperature were measured in early April on a number of first-year ice cores extracted through Anaktalak Bay, along the potential shipping route to Voisey's Bay Nickel Mine.

Institute for Marine Dynamics (1997) – depth profiles of the temperature and salinity of 10 first-year ice cores from the pack ice were measured during the *HENRY LARSEN* ice probe (Kirby, 1997). The field study was conducted in late March 1997 off Nain, Labrador. Air temperature, ice thickness and snow thickness were given.

Canadian Hydraulics Centre (2004) – conducted property measurements in landfast first-year ice near Nain in early February and late March (not yet published). Measurements included snow and ice thickness and depth profiles of the ice temperature and ice salinity. Borehole strength tests were conducted in March[2].

[2] Borehole strength data are currently being analyzed and will be reported in the report submitted in year 2 of the project. Property and *in situ* strength measurements were also made in April and May, but are currently being analyzed.

Ice property measurements from the above-mentioned sources were used to calculate the flexural strength of the ice using the intrinsic method (individual data markers shown in Figure 8). Measurements from Hebron Fjord (Gow, 1987) were not included in the figure because air and ice temperatures were not provided. Two solid lines were used to show the calculated flexural strengths for first-year ice at Hopedale and Resolute, calculated by the extrinsic method using the smoothed 30-yr MDT and mean ice thickness data. Plotting the flexural strength versus Julian Day resulted in a considerable amount of scatter, partly because the comparison does not allow for inter-annual variability in air temperatures.

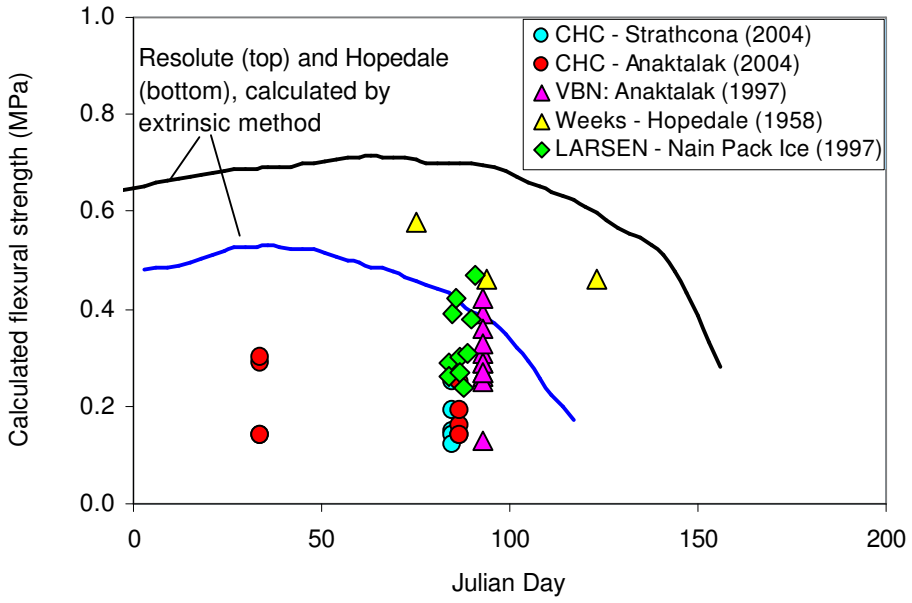

Figure 8 Calculated flexural strength, expressed in terms of Julian Day
(flexural strength calculated using extrinsic method – solid lines; intrinsic method –data markers)

Realizing that some of the scatter in Figure 8 resulted from inter-annual variability in air temperatures, the calculated flexural strength was plotted directly as a function of air temperature (Figure 9). Although plotting the results in this manner eliminated some of the scatter, there continues to be considerable variability in the flexural strengths for the same *study area* at the same *air temperature* (see the data markers for VBN and CHC). Results show that fluctuations in air temperature do not entirely explain the variability in flexural strengths observed in Figure 9. Although the calculated flexural strength of the ice decreased with increasing air temperature, there is no clear correlation between the two parameters.

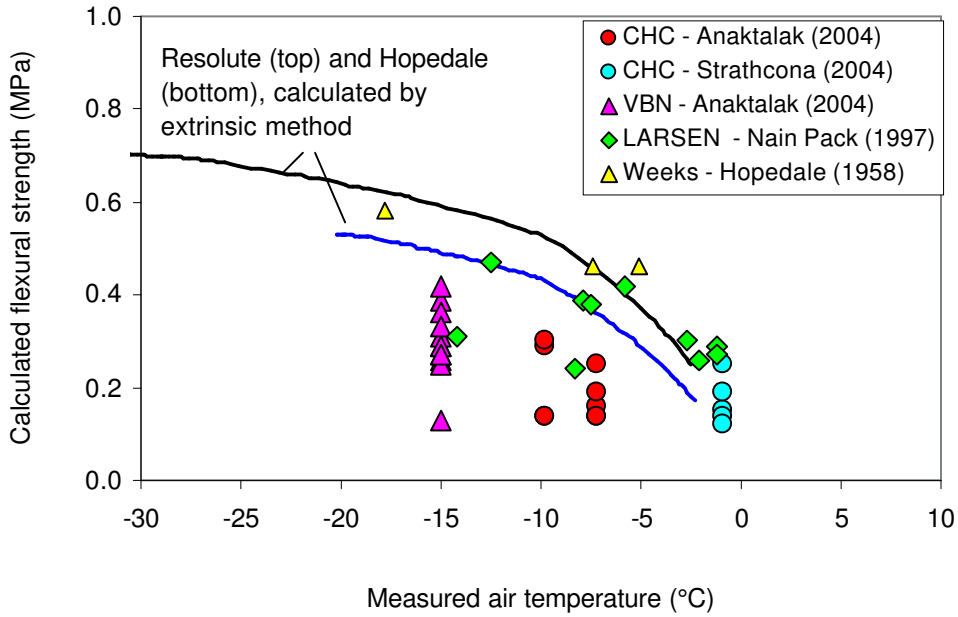

Figure 9 Calculated flexural strength, expressed in terms of air temperature
(data points – intrinsic method; solid lines – extrinsic method)

Since ice strength is directly related to ice temperature, the calculated strengths were plotted against bulk ice temperatures. For comparison purposes, previous measurements of the ice borehole strength of Arctic ice were plotted in the same figure. Results are shown in Figure 10, where the ice borehole strength is shown on the left axis (square data markers) and the calculated flexural strength is shown on the right axis. Results from Gow (1987) and Weeks and Lee (1958) are not included in the figure because the authors did not give information about ice temperatures.

Figure 10 shows that a direct correlation exists between the bulk ice temperature and ice strength. The ice borehole strength is particularly important in this regard - it is affected by, but measured independently of, the ice temperature. The same is not true for the calculated flexural strengths, since the bulk ice temperature was one of the input parameters required for the calculation. Results show that it is preferable to relate the ice strength to the bulk (depth-averaged) ice temperature directly rather than to some derivative of the air temperature.

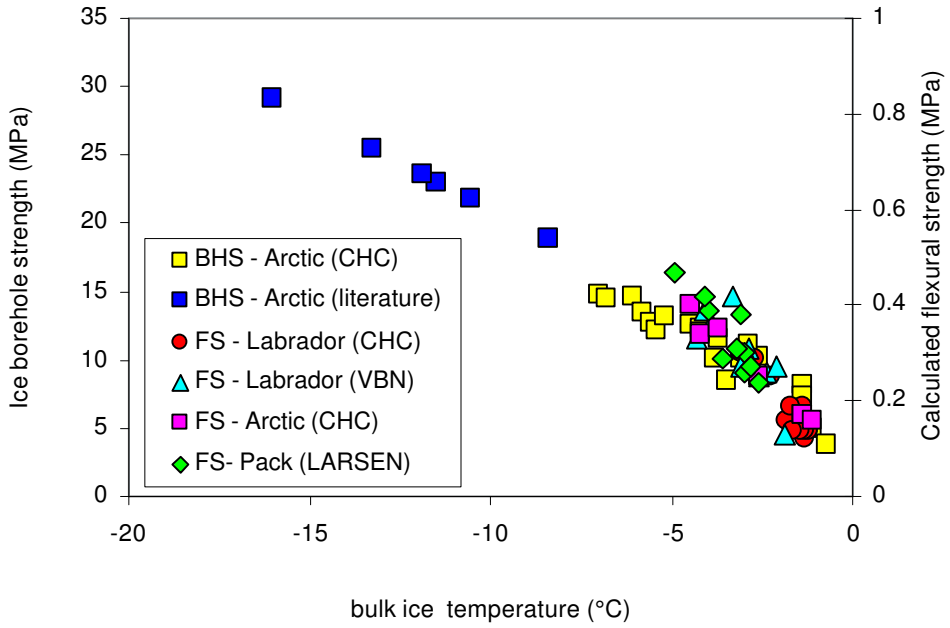

Figure 10 Ice borehole strength and flexural strength versus bulk ice temperature
(flexural strength (FS) was calculated using intrinsic method, using ice property measurements and borehole strength (BHS) was measured on level Arctic first-year ice)

7.0 Ice Strength Charts: Expressing Seasonal Changes in Strength

The ice strength algorithm for landfast first-year ice in the high Arctic used an exponential relation between the normalized ice strength and accumulated degree-days (Johnston and Timco, 2003-a). The strength output from the algorithm, and displayed on the preliminary Ice Strength Charts, was normalized to the maximum mid-winter flexural strength of Arctic first-year ice (0.71 MPa). Developing a specific algorithm for one location was considered appropriate for the high Arctic since it was based upon good agreement between the normalized flexural strength and the accumulated degree days. That methodology however, needed to be re-evaluated when considering ice at different latitudes.

7.1 Approaches for Displaying Strength on the Ice Strength Charts

Three different approaches were used to determine the most effective means of expressing the seasonal decrease in ice strength at different latitudes. The three approaches and their results are discussed below.

Case (i) - Ice Strength Normalized by mid-Winter Maximum of Arctic Ice Figure 11 shows the results of normalizing flexural strengths at different sites by the maximum mid-winter strength of Arctic first-year ice (0.71 MPa). Although this technique was appropriate for the strength algorithm developed for the high Arctic, it is not useful for ice outside the Arctic. One reason

for this is that many commercial vessels may not have experience with Arctic first-year ice. Normalizing the ice strength by some unfamiliar value would be irrelevant and would likely lead to confusion.

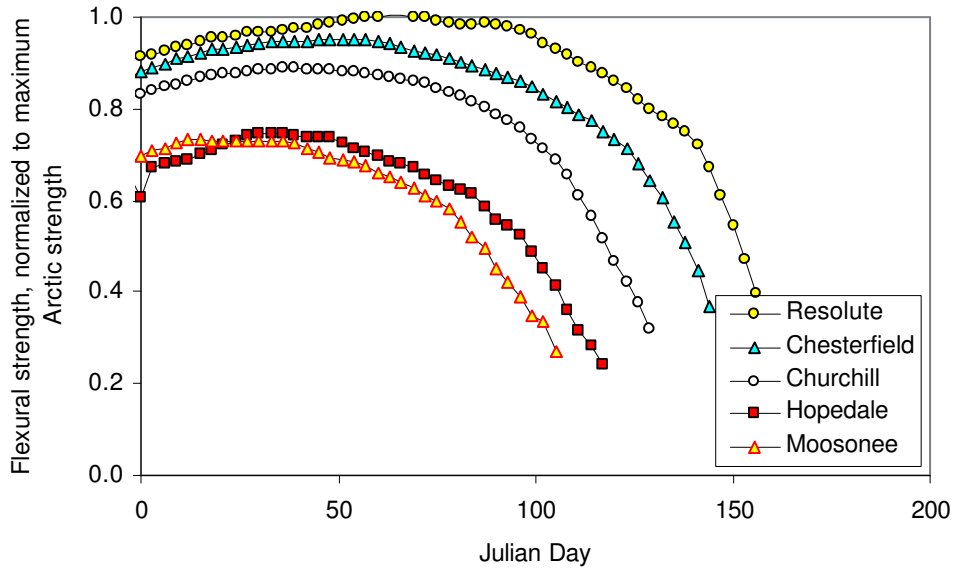

Figure 11 Flexural strength, normalized by mid-winter strength of Arctic ice

Case (ii) - Ice Strength Normalized by Site-Specific Maximum Using this approach, the strength at the different sites would be normalized by the maximum ice strength that occurs for that area. Based upon flexural strengths calculated using smoothed 30-yr MDT and mean ice thicknesseses, the following peak strengths would be used at the different sites:

Moosonee -	0.52 MPa
Hopedale -	0.53 MPa
Churchill -	0.63 MPa
Chesterfield -	0.67 MPa
Resolute -	0.71 MPa

This procedure is not recommended because it removes differences in ice strength for each site (Figure 12). In effect, normalizing by the site-specific maximum is misleading, since it gives the impression that there is little difference between the strength of first-year ice at the different latitudes. The variation in ice strength with latitude should be preserved.

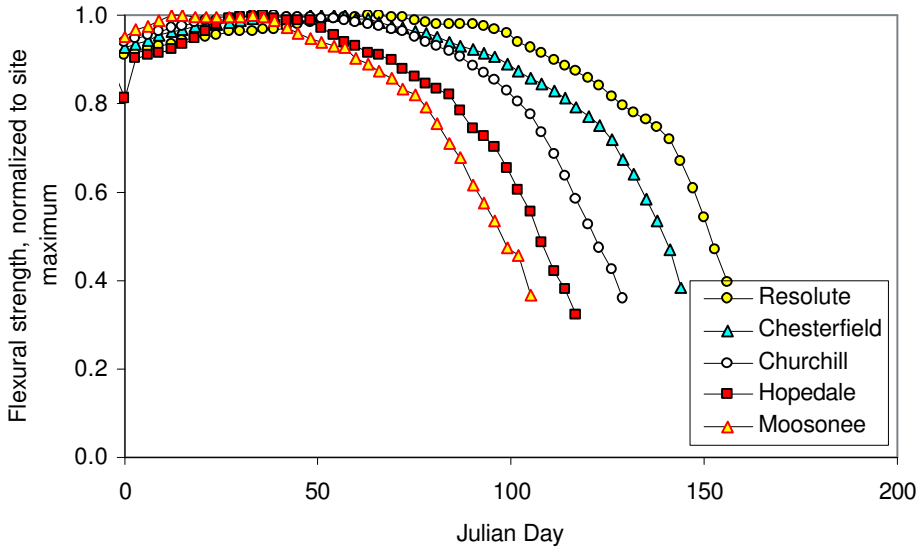

Figure 12 Flexural strength, normalized by maximum strength at each site

Case (iii) - Ice Strength Expressed in terms of its Physical Units Using physical units for the Ice Strength Charts has the advantage that it allows the end user to become familiar with a bona fide ice strength, rather than the dimensionless value that results from normalizing (Figure 13). In addition, it preserves differences in strength that are characteristic of ice at different latitudes.

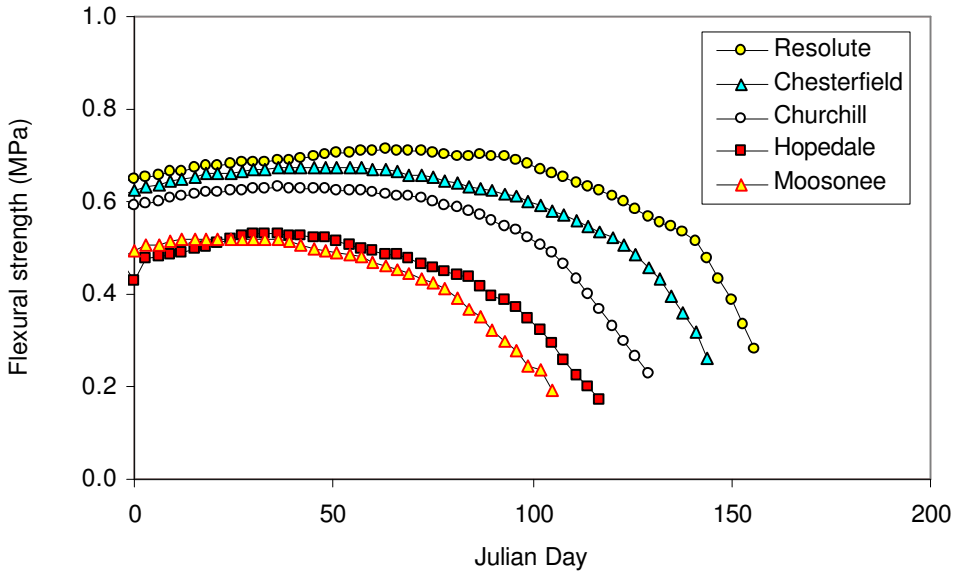

Figure 13 Flexural strength in terms of physical units

7.2 Relating Ice Strength to ADD

The strength algorithm that was developed for Arctic ice related the decrease in ice strength to the accumulated degree-days (ADD). That required two steps – (i) selecting an appropriate start date from which to begin accumulating degree days and (ii) establishing a baseline from which to reference accumulating degree days. A start date of March 1 and a baseline temperature of –30°C were appropriate for the high Arctic (Johnston and Timco, 2003-a).

The process of selecting a start date and baseline temperature for regions outside the Arctic made using the same approach for various regions extremely difficult. For example, a baseline of –35°C and a start date of January 1 would be needed to completely capture seasonal increases in temperature at all five selected sites. That procedure resulted in well-behaved curves when plotting accumulating degree days against Julian Day (Figure 14) but resulted in incoherent curves when the flexural strength was plotted against accumulated degree days (Figure 15).

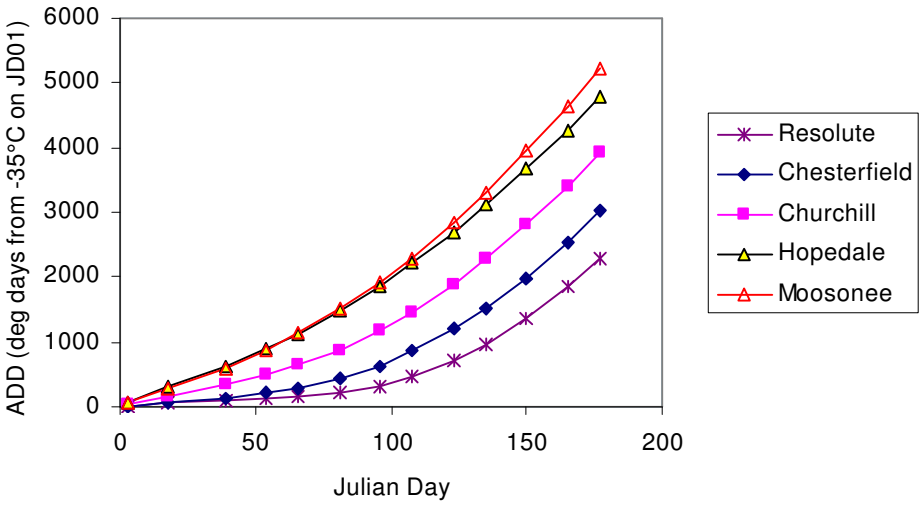

Figure 14 Accumulated degree-days from baseline of -35°C and start date of January 1

Using the same start date and baseline temperature for all five sites mistakenly indicated that ice in the Arctic (Resolute, Chesterfield, Churchill) began decreasing in strength earlier and at a much steeper rate than ice at southern latitudes. Based upon the relation between ice strength and ice temperature (illustrated in Figure 10), thinner ice in the sub-Arctic should decrease in strength sooner (and likely at a faster rate) than in the Arctic. Figure 15 shows the opposite trend, which illustrates why the decrease in ice strength should not be related to ADD. That is not a rational approach for comparing ice strengths at different latitudes.

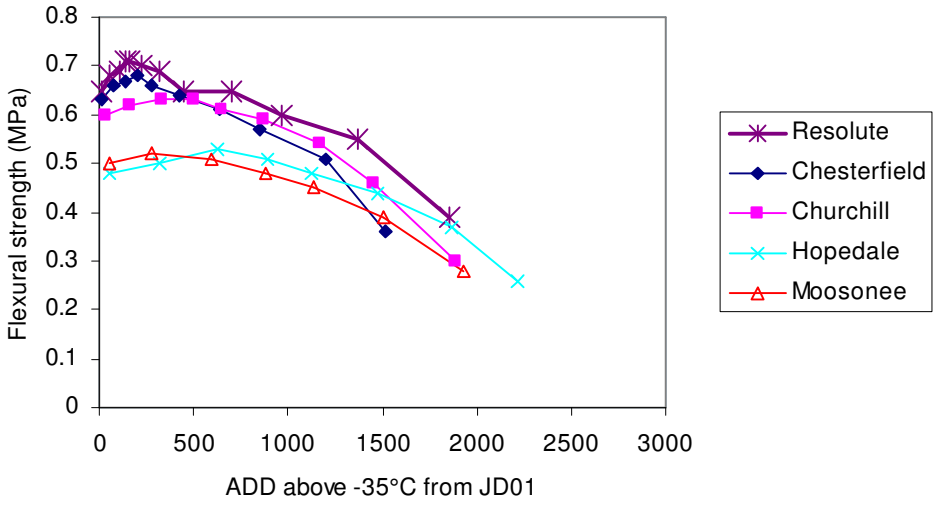

Figure 15 Seasonal decrease in ice strength as function of accumulated degree days

7.3 Charts Based upon the Flexural Strength Calculated Directly

The above discussion showed that relating the flexural strength to the accumulated degree days, based upon a standardized or flexible start date and baseline temperature, would not be appropriate for describing the decrease in strength that characterizes both sub-Arctic and Arctic ice. Rather, it is suggested that the flexural strength of the ice from different regions be calculated directly using the method developed by Timco and O'Brien (1994), as discussed below.

7.3.1 Extrinsic Method of Calculating the Flexural Strength: Equations

Since depth profiles of the ice temperature and ice salinity will not be available for all sites at all times, it will be necessary to calculate those parameters indirectly using known air temperatures (*T_air*) and estimated ice thicknesses (*h_i*). The air temperature and ice thickness will be used to calculate (a) *S* the bulk ice salinity, (b) *T_surface* the ice surface temperature, (c) *T_ice* a bulk ice temperature, (d) V_b a brine volume and (e) *FS* the flexural strength of the ice, as outlined in the following equations.

Salinity (ppt), *S*

for $h\_i < 0.34$ m
$S = 13.4 - 17.4\ (h\_i)$

for $h\_i > 0.34$ m
$S = 8 - 1.62\ (h\_i)$

Ice surface temperature (°C), *T_i-surface*

for *T_air* < -10°C
T_i-surface = 0.6 (*T_air*) – 4

for *T_air* < -10°C
T_i-surface = *T_air*

Bulk ice temperature (°C), *T_ice*

T_ice = (*T_i-surface* - 1.8)/2

Brine volume (ppt), V_b

for *T_ice* < -2.0°C
V_b = *S* ((49.185/ABS(*T_ice*)) + 0.532)

for *T_ice* > -2.0°C
Vb = 10000000000000

Flexural strength (MPa), *FS*

FS = 1.76 (exp(-5.88(sqrt(V_b/1000))

Table 3 showed that the extrinsic method of calculating the flexural strength from air temperature and estimated ice thickness data allows the ice strength at Moosonee to be determined until about the second week of April, and until the first week of June at Resolute. After that, the brine volume equation breaks down and the ice borehole strength must be used to document the seasonal decrease in ice strength. Since it has been suggested that the ice strength no longer be normalized, or related to the ADD, the borehole strength will need to be related to the flexural strength of the ice. That will require further study.

7.3.2 Effect of using MDT in Calculations

Determining the flexural strength from mean daily air temperatures requires making a decision about whether the mean daily temperatures (MDT) or a running average of the mean daily temperatures be used in the calculation. Figure 16 shows a comparison of the mean daily air temperatures for Resolute during 2002, the 7-day average of the 2002 mean daily temperatures and the two-week smoothed 30-yr mean daily temperatures. As might be expected, the 30-yr MDT all but eliminates day-to-day fluctuations in mean daily temperatures.

Figure 17 shows the effect of using the 2002 mean daily temperatures in the calculations – daily fluctuations in air temperature, although attenuated, are reflected in the calculated ice strength. Presently, there is little information about how quickly the ice responds to changes in air temperatures and the effect that it has on the ice strength. In order to determine whether the mean daily air temperature (or some average of it) should be used to calculate the flexural strength, work will need to be conducted on how quickly the ice responds to fluctuations in air temperature, and to what ice depth those changes occur. It is probable that, because of its thickness, Arctic first-year ice responds more slowly to those changes than sub-Arctic ice. The effect of an overlying snow cover will also factor in to the response time of the ice.

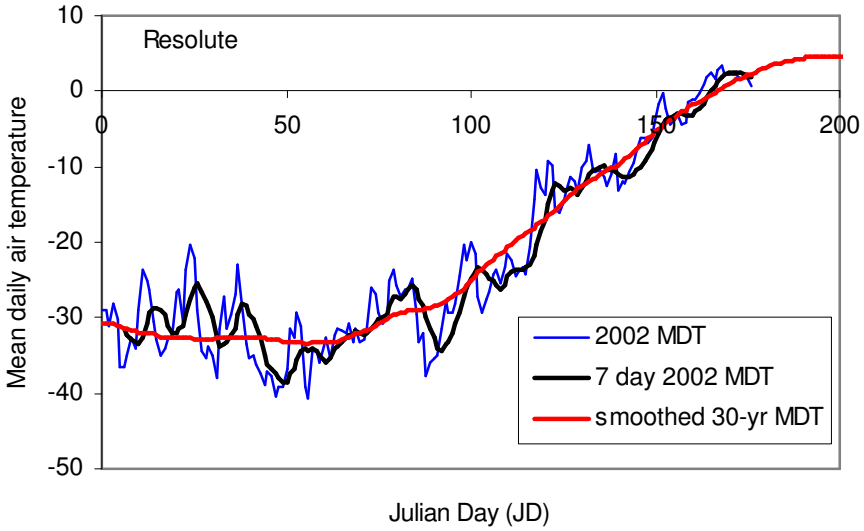

Figure 16 2002 MDT, 7-day ave of 2002 MDT and the 2-week smoothed 30-yr MDT

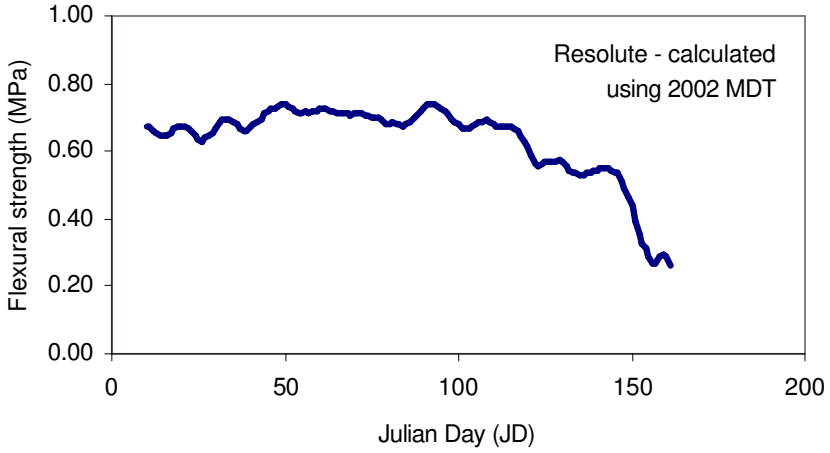

Figure 17 Calculated flexural strength for Resolute using 2002 MDT

7.4 Mapping Ice Strength

The regional flexural strengths plotted in Figure 7 were overlaid on a map twice each month from February to May, as shown in Figure 18. The strength map provides a means of visualizing the spatial variability in ice strength and the type of strength contours that future Ice Strength Charts might show. The bi-monthly strengths are listed in Table 4.

Figure 18 and Table 4 include data for the period over which the Timco and O'Brien technique is valid. Obtaining strength data beyond that point would require conducting borehole strength tests. Those data, although already available for the high Arctic, will soon be available for landfast first-year ice along the Labrador Coast. Results have shown that the ice borehole strength and flexural strength complement one another very well, since both exhibit similar seasonal decreases in strength. A relation between the two different strengths needs to be developed before one of the strengths, or both, can be used as a basis for future Ice Strength Charts.

Table 4 Bi-monthly Calculated Flexural Strengths for Selected Sites

Date	JD	Resolute	Chesterfield	Churchill	Hopedale/Nain	Moosonee
Feb 8	39	0.69	0.67	0.63	0.53	0.51
Feb 20	51	0.71	0.68	0.63	0.51	0.48
Mar 6	66	0.71	0.66	0.61	0.48	0.45
Mar 21	81	0.70	0.64	0.59	0.44	0.39
Apr 5	96	0.69	0.61	0.54	0.37	0.28
Apr 17	108	0.65	0.57	0.46	0.26	--
May 2	123	0.60	0.51	0.30	--	--
May 14	135	0.54	0.39	--	--	--
May 29	150	0.39	--	--	--	--
June 14	165	--	--	--	--	--

Feb 8 / Feb 23

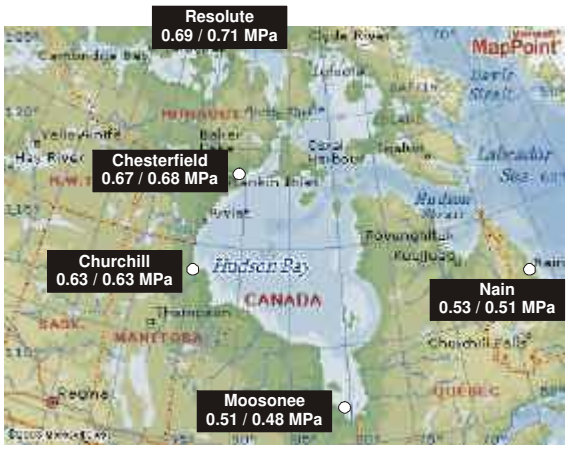

(a) February

Mar 7 / Mar 22

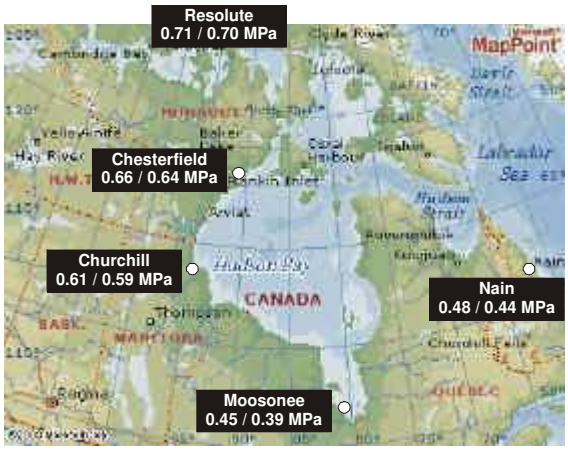

(b) March

Apr 6 / Apr 18

(c) April

May 3 / May 15

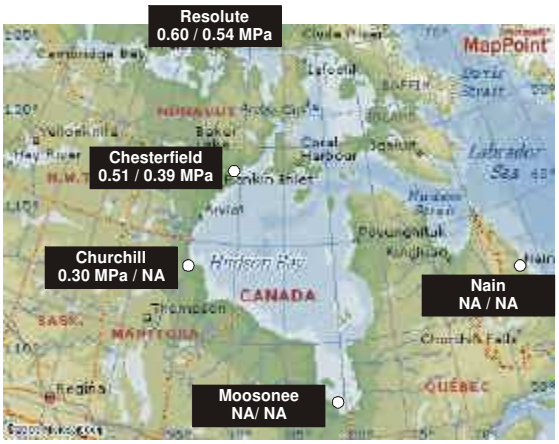

(d) May

May 30 / Jun 14

(e) May and June

Figure 18 Calculated flexural strength of first-year ice from February to June

8.0 Conclusions

This report summarized the work that has been done on developing a methodology for including level, landfast first-year ice in the sub-Arctic into the Ice Strength Charts issued by CIS. Previously, Ice Strength Charts only encompassed the high Arctic therefore a considerable amount of work was needed before a feasible approach for incorporating sub-Arctic ice into the Strength Charts could be determined.

Past Ice Strength Charts were issued from May to August and were based upon normalizing the calculated flexural strength of the ice and the measured ice borehole strength by their mid-winter maximums (Johnston and Timco, 2003-a). The calculated flexural strength was normalized by 0.71 MPa and the borehole strength was normalized by a value of 29 MPa – values that corresponded to the maximum strengths of Arctic first-year ice in mid-winter. This study showed that basing Strength Charts on a normalized ice strength would not be appropriate when incorporating both Arctic and sub-Arctic areas in the Charts. The problem related to selecting appropriate values by which to normalize the flexural and borehole ice strengths, since whatever normalizing factors were selected would not have been appropriate for ice in all regions. Nor will that value be familiar to all Commanding Officers, since the ships operate in very different ice conditions. It is suggested that if future Ice Strength Charts are to incorporate sub-Arctic ice, ice strengths have physical units (kPa or MPa).

The Ice Strength Algorithm for the high Arctic related the normalized ice strength to a derivative of the air temperature, the accumulated degree days, with respect to a pre-determined baseline. That baseline was selected with the objective of completely capturing the seasonal warming of the ice, while minimizing the effect that subzero air temperatures had on the accumulating degree days for each area. The selected baseline temperature was used to determine the number of accumulated degree days that corresponded to the date on which the ice strength had been measured (or calculated). The ice strength was then plotted against the accumulated degree days, and the relation between the two parameters was described using an exponential equation – the so-called Ice Strength Algorithm.

This study showed that neither the previously developed Strength Algorithm nor the technique used to obtain it, were appropriate for comparing ice strengths at different latitudes. In fact, the premises that were used to develop a Strength Algorithm for the high Arctic (relating the ice strength to the accumulated degree days) led to misleading results when the same technique was applied to sites at other latitudes. Relating the strength to the accumulated degree days erroneously implied that Arctic ice decreased in strength before sub-Arctic ice. It was concluded that Ice Strength Charts for Arctic and sub-Arctic ice should rely upon direct calculations of the flexural strength of the ice, using the Timco and O'Brien (1994) technique.

Timco and O'Brien (1994) describe two approaches for calculating the flexural strength of the ice. The first, more accurate, approach uses the measured ice temperature and salinity. The second approach uses known information about the air temperature and ice thickness. Since it is not always possible, or practical, to measure the properties of ice, it is suggested that the Ice Strength Charts use flexural strengths calculated by the second technique (from air temperatures and estimated ice thicknesses).

The suggestion that future Ice Strength Charts display the flexural strengths that retain their physical units would be feasible up to a certain date. As the ice decays, its temperature and brine volume increase. Both approaches developed by Timco and O'Brien (1994) are valid until the square root of the brine fraction exceeds 0.5. Once that happens, the equations break down and the flexural strength can no longer be calculated. Herein lies the usefulness of the borehole jack: it can be used to measure ice strength when the flexural strength cannot be calculated. Past work has shown that, where there is data overlap, the flexural strength and the ice borehole strength show similar seasonal decreases.

Having data on the borehole strength of ice in the Arctic enabled CIS to construct Ice Strength Charts for the high Arctic after mid-June, when the flexural strength could no longer be calculated. To date, borehole strengths have only been measured on decaying first-year ice in the high Arctic. Results will soon be available from borehole strength tests that were recently conducted in landfast first-year ice off the Labrador coast. Year two of this project will use the knowledge gained from the Labrador ice to infer ice conditions in Hudson Bay and to determine whether sub-Arctic ice shows the same trend of decreasing strength observed in Arctic ice.

Since it is suggested that future Ice Strength Charts calculate the ice strength directly using known air temperatures and estimated ice thickness, using the borehole jack as a proxy for the decrease in ice strength will require developing a direct relation between the flexural strength and the borehole strength of the ice. To date, no such relation has been developed. However, work has been done to relate the ice borehole strength to the confined compressive strength of ice that was measured in a laboratory (Sinha, 1986) and to the ice strength measured during unconfined compression tests (Masterson, 1996; Sinha, 1986).

This study showed a direct relation between measured ice borehole strength and the measured bulk ice temperature (depth-averaged). Similar results were obtained when the calculated flexural strength was plotted against the bulk ice temperature[3]. Using the bulk ice temperature to indicate ice strength underscores the importance of relating known air temperatures to bulk ice temperatures. This 'not-so-straightforward' relation becomes even more complicated when a dry or wet snow cover blankets the ice. Timco and O'Brien (1994) make assumptions about the effect that an overlying snow cover has in attenuating temperature changes in the ice, however this is an area that deserves further attention. This is especially true considering that the snow cover in sub-Arctic regions experiences changes almost daily, unlike the relatively stable snow pack in the Arctic. As a first approach, the technique developed by Timco and O'Brien (1994) can be used to calculate the flexural strength, however the influence that snow has on the ice temperature (hence ice strength) should be examined.

If future Strength Charts are to use air temperatures to calculate the flexural strength of the ice, a decision should be made as to which type of averaging would be appropriate for the air temperatures output by CIS's GEM model. In this report, the two-week smoothed average of the 30-year normal mean daily temperatures (MDT) were used to calculate the flexural strength of the ice. Results showed these air temperatures do not have the regional, interannual

[3] The two variables were not independent of one another, however, since ice temperature was an input for the calculations.

variability although, at present, it is not known how much that variability affects ice strength, in the short term. Before an air temperature is selected for strength calculations, attention should be given to examining the response time of the ice to changes in air temperature, and how those temperature changes affect its ice strength. Once that has been done, it would be possible to select the air temperature that is most appropriate for calculating the flexural strength of the ice.

This study focused upon developing a technique for incorporating level, landfast first-year ice in the sub-Arctic into future Ice Strength Charts. The properties of decaying landfast ice in the Arctic have been measured for three years and, after this year, will have been measured for one year in the sub-Arctic. It would be of interest to relate measurements of landfast first-year ice to measurements made in pack ice. Work is currently being performed in rubbled ice off Labrador. Those results could be used to understand how the properties of first-year ice embedded in pack ice differs from landfast ice.

9.0 Summary

A number of suggestions about incorporating sub-Arctic ice into future Ice Strength Charts were put forth. The study also recommended areas in which future work should be directed to enhance understanding of how the ice responds to environmental changes and the impact that those changes have on ice strength. That information would lead to improved Ice Strength Charts. The suggestions are summarized below:

- If the Ice Strength Charts are to incorporate sub-Arctic ice, the ice strength should be expressed in physical units rather than normalized by a maximum strength.

- Ice Strength Charts that include Arctic and sub-Arctic ice should rely upon direct calculations of the flexural strength using the Timco and O'Brien (1994) approach. That requires data on air temperatures and estimated ice thicknesses.

- Using the ice borehole strength as a proxy for the flexural strength (beyond where it can be calculated) requires developing a direct relation between the two strengths.

- The influence that snow cover has on the bulk ice temperature, hence ice strength, is very important and should be examined.

- Attention should be given to quantifying the response time of the ice to short term changes in air temperature, and its implications for ice strength.

- A first look at relating the properties of landfast first-year ice to first-year ice in the transition zone is possible using recently acquired data on rubbled ice off the Labrador Coast.

10.0 Acknowledgments

Financial support for this project was provided by Canadian Ice Service. That assistance is most appreciated. Transport Canada and Canadian Ice Service sponsored the field program that was conducted in the landfast ice off the Labrador Coast. Many thanks to both departments for their continued support and interest in this area.

11.0 References

Bilello, M.A. (1960) Formation, Growth and Decay of Sea Ice in the Canadian Arctic Archipelago. U.S. Army Snow Ice and Permafrost Research Establishment Corps of Engineers. Research Report 65

Bilello, M.A. (1980) Maximum Thickness and Subsequent Decay of Lake, River and Fast Sea Ice in Canada and Alaska. U.S. Army Cold Regions Research and Engineering Laboratory, Hanover, New Hampshire.

Bilello, M.A. and Lunardini, V.J. (1996) Ice Thickness Observations, North American Arctic and Subarctic, 1974 – 75, 1975 – 76 and 1976 – 77. CRREL Special Report. No. 43, IX. May, 1996. 221 pp.

Bilello, M.A. and R.E. Bates (1991) Ice Thickness Observations: North American Arctic and Subarctic, 1972-73 and 1973-74. Special Report 43, VIII. U.S. Army Cold Regions Research and Engineering Laboratory, Hanover, New Hampshire.

Cormorant Ltd. (1997) Voisey's Bay Ice Monitoring Program: Program Report. Prepared for Voisey's Bay Nickel Company Limited, St. John's, Newfoundland.

Gow, A.J. (1987) Crystal structure and salinity of sea ice in Hebron Fiord and vicinity, Labrador. U.S. Army Cold Regions Research and Engineering Laboratory, Hanover, New Hampshire.

Johnston, M., Frederking, R. and Timco, G. (2002) Properties of Decaying First Year Sea Ice: Two Seasons of Field of Field Measurements. Proceedings 17th International on Okhotsk Sea and Sea Ice, Mombetsu, Hokkaido, Japan, pp. 303-311.

Johnston, M. and Timco, G. (2003-a) Developing an Ice Strength Algorithm for Level, Landfast First-year ice in the High Arctic. Technical report issued by Canadian Hydraulics Centre for Canadian Ice Service, March 2003, Ottawa, Ontario, CHC-TR-013, 21 p.

Johnston, M., Frederking, R. and Timco, G. (2003-b) Properties of Decaying First-year Sea Ice at Five Sites in Parry Channel. Proceedings 17th International Conference on Port and Ocean Engineering under Arctic Conditions, POAC'03, Trondheim, Norway, Vol. 1, pp. 131-140.

Kirby, C. (1997) Voisey's Bay Ice Probe 1997 on CCGS HENRY LARSEN. Report issued by Institute for Marine Dynamics of the National Research Council, submitted to the Canadian Coast Guard, TR-1997-26, September, 1997, 9 p.

Masterson, D. (1996) Interpretation of *In Situ* Borehole Ice Strength Measurement Tests. *Can. J. Civ. Eng*. Vol. 23. pp. 165- 179.

Sinha, N. K. (1986) The Borehole Jack: Is it a Useful Tool? Proc. of 5th Int. Offshore Mechanics and Arctic Engineering Symp. (OMAE). Tokyo, Japan. 13 – 17 April 1986. Vol. IV. pp. 328 – 335.

Timco, G. and Frederking, R. (1990) Compressive Strength of Sea Ice Sheets. Cold Regions Science and Technology, No. 17, pp. 227 - 240.

Timco, G. and O'Brien, S. (1994) Flexural Strength Equation for Sea Ice. Jour. Cold Regions Science and Technology, Vol. 22, pp. 285 – 298.

Weeks, W.F. and Lee, O.S. (1958). Observations on the Physical Properties of Sea-Ice at Hopedale, Labrador. Arctic, Vol. 11(3), pp. 135-155. September 1958. Canada.

Appendix A: Literature Review

REFERENCES

1. Barber, F.G and M.M. Larnder (1968). The Water and Ice of Hudson Bay. in Science, History and Hudson Bay Vol. 1 Edited by C.S. Beals, pp. 318-341. Dept of Energy, Mines and Resources, Ottawa.
2. Belliveau, D.J., C.L. Tang, and A.M. Mahon (1998). Measurement of Ice Growth and Melt in the Labrador Pack Ice. Proceedings of the Eighth (1998) International Offshore and Polar Engineering Conference, Vol. 3, pp. 36-41. Montreal, Canada, May 24-29, 1998.
3. Berenger, D. and B.D. Wright (1980). Ice Conditions Affecting Offshore Hydrocarbon Production in the Labrador Sea. Intermaritec 80 Int. Conference on Marine Sciences and Ocean Engineering. IMT 80-203 Hamburg
4. Bilello, M.A. (1960). Formation, Growth and Decay of Sea Ice in the Canadian Arctic Archipelago. U.S. Army Snow Ice and Permafrost Research Establishment Corps of Engineers. Research Report 65.
5. Bilello, M.A. (1980). Maximum Thickness and Subsequent Decay of Lake, River and Fast Sea Ice in Canada and Alaska. U.S. Army Cold Regions Research and Engineering Laboratory, Hanover, New Hampshire.
6. Bilello, M.A. and R.E. Bates (1991). Ice Thickness Observations: North American Arctic and Subarctic, 1972-73 and 1973-74. Special Report 43, VIII. U.S. Army Cold Regions Research and Engineering Laboratory, Hanover, New Hampshire.
7. Canadian Coast Guard (1998). Final Report: Voisey's Bay Ice Probe. March.
8. Carsey, F.D., S.A. Digby Argus, M.J. Collins, B. Holt, C.E. Livingstone and C.L. Tang (1989). Overview of LIMEX'87 Ice Observations. IEEE Transactions on Geoscience and Remote Sensing, Vol. 27, No. 5, September 1989.
9. Catchpole, A.J.W. and M.-A. Faurer (1983). Summer Sea Ice Severity in Hudson Strait, 1751-1870. Climatic Change Vol. 5 (2) pp. 115-139.
10. Centre for Cold Ocean Resources Engineering (1977). Meteorological Ground Truthing, Hopedale. Field Data Report No. 5. C-CORE Publication 77-34.
11. Centre for Cold Ocean Resources Engineering (1977). Ice Characterization, Hopedale. Field Data Report No. 6. C-CORE Publication 77-35.
12. Centre for Cold Ocean Resources Engineering (1977). Additional Ground Truth Measurements, Hopedale. Field Data Report No. 7. C-CORE Publication 77-36.
13. Centre for Cold Ocean Resources Engineering (1977). Ground Truth Measurements, Goose Bay. C-CORE Field Data Report No.9. Publication 77-38.
14. Centre for Cold Ocean Resources Engineering (1979). Project SAR '77 Summary Report. C-CORE Publication 79-15.
15. Cormorant Ltd. (1997). Voisey's Bay Ice Monitoring Program: Program Report. Prepared for Voisey's Bay Nickel Company Limited, St. John's, Newfoundland.
16. Cormorant Ltd. (1998). Voisey's Bay Ice Monitoring Program: Component Project Data Report 1. Landfast Ice Thickness Measurements Along the Voisey's Bay Potential Shipping Route. Prepared for Voisey's Bay Nickel Company Limited, St. John's, Newfoundland. 3 August 1998.
17. Danielson, E.W. (1971). Hudson Bay Ice Conditions, Arctic 27 (2), pp. 90-106.
18. DF Dickens Associates Ltd. (1997). Review of Historical Ice Conditions Affecting the Voisey's Bay Development. Prepared for Voisey's Bay Nickel Company Limited, St. John's, Newfoundland.

19. DF Dickens Associates Ltd. (1997). Voisey's Bay 1996 Environmental Baseline Technical Data Report: Spring Ice Break-Up Survey. Prepared for Voisey's Bay Nickel Company Limited, St. John's, Newfoundland.
20. Environment Canada (1974). Ice summary and analysis 1971 Hudson Bay and approaches 43 p.
21. FENCO (1977). Winter Field Ice Survey Offshore Labrador, 1977. Prepared for TOTAL Eastcan Exploration Ltd, Calgary, Alberta.
22. Freeman, N.G., J.C. Roff, and R.J. Pett (1982). Physical, chemical and biological features of river plumes under an ice cover in James and Hudson's Bays. Nat. Can. Que., 109, pp. 745-764.
23. Godin, G. (1986). Modification by an ice cover of the tide in James Bay and Hudson Bay. Arctic, 39: p 65-67.
24. Gow, A.J. (1987). Crystal structure and salinity of sea ice in Hebron Fiord and vicinity, Labrador. U.S. Army Cold Regions Research and Engineering Laboratory, Hanover, New Hampshire.
25. Ingram, R.G. and P. Larouche (1987). Variability of an under-ice river plume. J. Geophys. Res. 92, pp. 9541-9547.
26. Langleben, M.P. (1959) Some Physical Properties of Sea Ice II. Can. J. Phys. Vol. 37.
27. Langleben, M.P. (1972) Decay of an annual cover of sea ice. Journal of Glaciology, 11(63), p 337- 344.
28. Larnder, M.M. (1968). The ice. in Science, History and Hudson Bay, Part 1, edited by C.S. Beals, pp. 318-341. Dept of Energy, Mines and Resources, Ottawa.
29. Larouche, P. and P.S. Galbraith (1989). Factors Affecting Fast-Ice Consolidation in Southeastern Hudson Bay, Canada. Atmosphere-Ocean, Vol. 27 (2), pp. 367-375. Canadian Meteorological and Oceanographic Society.
30. LeDrew, B.R. and S.T. Culshaw (1977). Ship-in-the-Ice Data Report. Centre for Cold Ocean Resources Engineering, St. John's, Canada. C-CORE Publication No. 77-28.
31. Lepage, S. and R.G. Ingram (1991). Variation of Upper Layer Dynamics During Breakup of the Seasonal Ice Cover in Hudson Bay. Journal of Geophysical Research, Vol. 96, No. C7, pp. 12,711- 12,724, July 15, 1991.
32. Loset, S., A. Langeland, B. Bergheim & K.V. Hoyland (1998). Geometry and physical properties of a stamucha found on Spitsbergen. Proceedings of the 14th International Symposium on Ice (IAHR), Vol. 1, pp. 339-344. July 27-31, 1998.
33. Martinson, C.R. (1985). Impulse radar sounding of level first-year sea ice from an icebreaker. U.S. Army Cold Regions Research and Engineering Laboratory, Hanover, New Hampshire.
34. McKenna, R. L. (1989). Section 8.7: Ice Mechanical Properties. LIMEX'89 Data Report. Energy, Mines and Resources Canada.
35. Moore, B.D.H. and A.F. Gregory (1979). Monitoring and Mapping Sea-Ice Breakup and Freezeup of Arctic Canada from Satellite Imagery. Arctic and Alpine Research, Vol. 11(2), pp. 229-242.
36. Peterson, I.K. (1990). Sea ice velocity fields off Labrador and eastern Newfoundland derived from satellite imagery: 1984-1987. Can. Tech. Rep. Hydrogr. Ocean Sci. No. 129:vi, 85 p.
37. Pounder, E. R. and E. M. Little (1959). Some Physical Properties of Sea Ice I. Can. J. Phys. Vol. 37.

38. Prinsenberg, S.J. (1980). Man-made changes in the freshwater input rates of Hudson and James Bays. Can. J. Fish. Aquat. Sci., Vol. 37, pp. 1101-1110.
39. Prinsenberg, S.J. (1986). Man-made changes in the freshwater input rates of Hudson and James Bays. in Canadian Inland Seas by I.P. Martini, pp. 163-186.
40. Prinsenberg, S.J. (1987). Seasonal Current Variations Observed in Western Hudson Bay. Journal of Geophysical Research, Vol. 92, No. C10, pp. 10756-10766, September 15, 1987.
41. Prinsenberg, S.J. (1988). Ice-cover and ice-ridge contributions to the freshwater contents of Hudson Bay and Foxe Basin. Arctic, Vol. 41, pp. 6-11.
42. Prinsenberg, S.J. and I.K. Peterson (1992). Sea-Ice Properties off Labrador and Newfoundland During LIMEX '89. Atmosphere-Ocean, Vol. 30 (2), pp. 207-222. Canadian Meteorological and Oceanographic Society.
43. Raney, R.K., S. Digby Argus and L. NcNutt (1989). Labrador Ice Margin Experiment LIMEX'89; An Overview. IGARSS Int. Geosci. and Remote Sensing Symp. Vol. 3 Part 3, p 1517-1519.
44. Rescan Environmental Services Limited (1997). Physical Oceanography of the Voisey's Bay Project Area- Voisey's Bay Nickel Company Environmental Impact Assessment. Prepared for Voisey's Bay Nickel Company Limited, St. John's, Newfoundland. November 1997.
45. Steel, A., J.I. Clark and P. Morin (1994). A comparison of pressuremeter test results in sea ice. Canadian Geotechnical Journal, Vol. 31, No. 2, pp. 254-260.
46. Tan, F.C. and P.M. Strain (1996). Sea ice and oxygen isotopes in Foxe Basin, Hudson Bay and Hudson Strait, Canada. Journal of Geophysical Research, Vol. 101 (C9), pp. 20869-20876.
47. Transportation Development Centre (1985). Trials off the Labrador Coast May 1984, Transport Canada. Edited by: R. Frederking and J.E. Laframboise. Polarstern: Report from the Canadian Team. May 1985.
48. Veitch, B., P. Kujala, P. Kosloff and M. Lepparanta (1991). Field Measurements of the Thermodynamics of an Ice Ridge. Helsinki University of Technology, Faculty of Mechanical Engineering, Laboratory of Naval Architecture and Marine Engineering.
49. Wang, J., L.A. Mysak and R.G. Ingram (1994). Interannual Variability of Sea-Ice Cover in Hudson Bay, Baffin Bay and Labrador Sea. Atmosphere Ocean, Vol. 32 (2) 1994, pp. 421-447. Canadian Meteorological and Oceanographic Society.
50. Weeks, W.F. and O.S. Lee (1958). Observations on the Physical Properties of Sea-Ice at Hopedale, Labrador. Arctic, Vol. 11(3), pp. 135-155. September 1958. Canada.
51. Winsor, W.D., G.B. Crocker, R.F. McKenna, and C.L. Tang (1990). Sea Ice Observations during LIMEX, March - April 1989. Canadian Data Report of Hydrography and Ocean Sciences No. 81: iv, 43 p.

Barber, F.G and M.M. Larnder (1968). The Water and Ice of Hudson Bay. in Science, History and Hudson Bay Vol. 1 Edited by C.S. Beals pp. 318-341. Dept of Energy, Mines and Resources, Ottawa.

This chapter describes some of the physical features of the water of Hudson Bay and the influences that determine them. The region is still only imperfectly known, so much of the discussion is based on experience and understanding gained in study of other regions, both coastal and oceanic. This approach is possible because Hudson Bay is intimately connected to the North Atlantic Ocean, which in turn is a significant part of the world ocean. For a number of reasons one may expect to find unique features in the Bay: its shallowness relative to the total area, its continental location, the fact that it is ice covered in winter but not in summer, and the very high tides that occur in certain areas.

Belliveau, D.J., C.L. Tang, and A.M. Mahon (1998). Measurement of Ice Growth and Melt in the Labrador Pack Ice. Proceedings of the Eighth (1998) International Offshore and Polar Engineering Conference, Vol. 3, pp. 36-41. Montreal, Canada, May 24-29, 1998.

Ice growth and melt play a major role in the length of time the yearly offshore pack ice impact on shipping, fishing and offshore petroleum development. This paper describes an automated acoustic system that will monitor the growth and melt of ice and transmit its data via satellite. System design, calibration and results from three deployments are presented.

Berenger, D. and B.D. Wright (1980). Ice Conditions Affecting Offshore Hydrocarbon Production in the Labrador Sea. Intermaritec 80 Int. Conference on Marine Sciences and Ocean Engineering. IMT 80-203 Hamburg

Recent exploratory drilling on Canada's Labrador Shelf has been encouraging and production feasibility studies are currently underway. However, the production of hydrocarbon reserves from this area will require unique solutions to the problems associated with its hostile environment. Because of this, extensive research has been carried out to define the environmental constraints and to determine design criteria for offshore production systems. A major factor affecting the design of these systems is the ice regime of the Labrador Sea, comprised of icebergs and a seasonal sea ice cover.

Here, ice conditions in the Labrador Sea are described and the results of sea ice and iceberg research programs carried out by the Labrador Group since the early 1970's are highlighted. The sea ice studies include field data acquisition on the physical and mechanical properties of first and multi-year ice present in the area along with its movement. The iceberg information, collected in conjunction with the exploratory drilling program, consists of data on the physical properties of icebergs and their motion characteristics. The large variability in ice conditions is shown to be a significant factor affecting the design of offshore hydrocarbon production systems for the Labrador Sea.

Bilello, M.A. (1960). Formation, Growth and Decay of Sea Ice in the Canadian Arctic Archipelago. U.S. Army Snow Ice and Permafrost Research Establishment Corps of Engineers. Research Report 65. July 1960.

Freeze-up at Alert, Eureka, Isachsen, Mould Bay, and Resolute in the Canadian Arctic was observed to occur any time between the last week in August and the last week in September. A mathematical relationship between air temperature and sea-ice formation provided a favorable method for predicting the date of freeze-up at these stations.

The maximum seasonal growth of sea ice, 269 cm, was measured at Isachsen; the minimum, 149 cm, was measured at Resolute. These values are based on measurements made at the five stations in the Canadian Arctic Archipelago having a total of 35 station years of record. Equations to predict the growth of sea ice by increments were derived empirically from the observations made at these

locations. A separate term is introduced in the equations to take account of the effects of snow-cover depths on ice growth. To apply the formulas only air-temperature and snow-depth data are required.

The study disclosed good correlation between air temperature and decrease in sea-ice thickness at the Arctic stations. The relationship was found to be:

$$h = 0.55 \Sigma\theta$$

where h = decrease in ice thickness (cm) and $\Sigma\theta$ = accumulated degree days (above - 1. 8°C).

Bilello, M.A. (1980). Maximum Thickness and Subsequent Decay of Lake, River and Fast Sea Ice in Canada and Alaska. U.S. Army Cold Regions Research and Engineering Laboratory, Hanover, New Hampshire. February 1980.

Report provides a description of weekly measurements of ice thickness and reports of ice surface conditions at the regional distribution of ice observing stations in the arctic and subarctic. In this study, the portion of data relating to maximum ice thickness and subsequent decay collected from this North American network is presented and examined. Included in the report are 1) tabulations of the weekly ice thickness measurements and observations of ice conditions, 2) a series of curves that show the rate of ice decay 3) a listing of the dates when the bodies of water studied become clear of ice and 4) an analysis of the rate of ice decay versus concurrent meteorological conditions. The investigation covers a period ranging from 3 to 16 winters and includes observations made at 40 stations in Canada and 26 stations in Alaska.

Bilello, M.A. and R.E. Bates (1991). Ice Thickness Observations: North American Arctic and Subarctic, 1972-73 and 1973-74. Special Report 43, VIII. U.S. Army Cold Regions Research and Engineering Laboratory, Hanover, New Hampshire. December 1991.

With the publication of this eighth report, which provides weekly data for the winters of 1972-73 and 1973-74, the series now provides 16 years of continuous information on seasonal ice. Considerable information on the ice formation, surface conditions, snow conditions, snow depths and ice breakup provided by the Canadian observers in their original reports is presented in the remarks columns of Tables I and II.

Canadian Coast Guard (1998). Final Report: Voisey's Bay Ice Probe. March 1998.

In late winter, 1997, the Canadian Coast Guard (CCG) conducted an ice probe to the Nain and Voisey's Bay regions of northern Labrador. A comprehensive measurement program, conducted from the *CCGS Henry Larsen,* included surveys of marine mammals and ice conditions, a comprehensive assessment of ship performance in pack ice and other scientific surveys.

Several partners jointly undertook this initiative along with the Canadian Coast Guard to maximize this unique scientific and research opportunity. These partners included Voisey's Bay Nickel Company (VBNC), the Innu Nation, the Labrador Inuit Association (LIA), Canadian Wildlife Service, Fisheries and Oceans, Science Branch, Oceanography and Marine Mammal, Environment Canada, Transport Canada and a number of specialist contractors. The Innu Nation and the LIA provided on board observers bringing their unique perspectives of the Labrador Coast.

Specialist contractors included the National Research Council Institute for Marine Dynamics (IMD), the Centre for Cold Ocean Resources Engineering (CCORE) and P.E. Dunderdale and Associates. The collaboration and shared findings of these various groups was a key success factor for the Voisey's Bay Ice Probe.

This report is divided into nine (9) sections. Sections three (3) through eight (8) is a complete compilation of all the data provided by the various partners and contractors. Section nine (9) is a list of the video tape taken on the voyage, due to the volume of tape taken a summary video has been prepared and accompanies this report.

Carsey, F.D., S.A. Digby Argus, M.J. Collins, B. Holt, C.E. Livingstone and C.L. Tang (1989). Overview of LIMEX'87 Ice Observations. IEEE Transactions on Geoscience and Remote Sensing, Vol. 27, No. 5, September 1989.

Ice observations, results and conclusions are summarized for the March 1987 Labrador Ice Margin Experiment, called LIMEX'87, an international oceanographic study conducted in the pack ice of the Grand Banks area off the coast of Newfoundland. Included are the ice extent, floe size and thickness, ice kinematics and rheology, ice microwave properties, oceanic properties under the ice, and penetration of swell into the ice.

Catchpole, A.J.W. and M.-A. Faurer (1983). Summer Sea Ice Severity in Hudson Strait, 1751-1870. Climatic Change Vol. 5 (2) pp. 115-139.

Annual indices of sea ice severity in Hudson Strait, for the period 1751 to 1870, are derived from written historical evidence contained in ships' log-books. These logs were all kept on Hudson's Bay Company ships sailing from London to the Company's trading posts. The log-books are homogeneous in nature and this property facilitates their numerical interpretation. The annual indices are subjected to face validity testing which indicates that they may plausibly be accepted as measures of sea ice severity. The results are examined in relation to the present day behaviour of sea ice in Hudson Strait and they provide evidence that the summer severity of ice conditions is mainly determined by atmospheric circulation conditions.

Centre for Cold Ocean Resources Engineering (C-CORE). Meteorological Ground Truthing, Hopedale. Field Data Report No.5 C-CORE Publication 77-34.

Project SAR '77 investigated the merit of a synthetic aperture radar system in the study of sea ice in the Labrador Sea area and on the east coast of Newfoundland. Ground truth information was collected at three field sites, being primarily concerned with meteorological observations and the physical properties of the ice sheet and snow cover.

This report summarizes relevant meteorological data collected by personnel working at the Hopedale Weather Station, under contract to the Atmospheric Environment Service of the Canadian Department of Environment. The data presented was obtained during the winter of 1977 in Hopedale, on the coast of Labrador.

Centre for Cold Ocean Resources Engineering (C-CORE). Ice Characterization, Hopedale. Field Data Report No.6 C-CORE Publication 77-35.

Project SAR '77 was conducted to investigate the merits of using a synthetic aperture radar system for the study of sea ice forms occurring in the Labrador Sea area and on the east coast of Newfoundland.

Radar flights were conducted over Hopedale on the east coast of Labrador. Ground truth information was collected prior to, and during these flights. Data was acquired on the physical properties of first year shorefast sea ice and snow cover adjacent to Hopedale. These measurements and observations are presented in this Field Data Report. A selection of the synthetic aperture radar imagery collected in the area is also presented and briefly discussed.

Centre for Cold Ocean Resources Engineering (C-CORE). Additional Ground Truth Measurements, Hopedale. Field Data Report No.7 C-CORE Publication 77-36.

Project SAR '77 investigated the merit of a synthetic aperture radar system in the study of sea ice in the Labrador Sea area and on the east coast of Newfoundland. Ground truth information was collected at three field sites, being primarily concerned with meteorological observations and the physical properties of the ice sheet and snow cover.

This report discusses additional data which may be used as ground truth information for the SAR data collected in the area of Hopedale on the coast of Labrador. The additional data presented in the report is in the form of 35 mm ground based photographs, 70 mm low and high altitude photographs,

and LANDSAT satellite imagery recorded in the mean infrared Band 7 of the multispectral scanner onboard the spacecraft.

The deployment of passive radar reflectors on fast ice seaward of Hopedale is also discussed.

Centre for Cold Ocean Resources Engineering (C-CORE). Ground Truth Measurements, Goose Bay. C-CORE Field Data Report No.9 Publication 77-38.

The operational headquarters for PROJECT SAR 77 was located at Goose Bay Airport. A series of tests were carried out at this site to provide information that would facilitate both the interpretation of the digital record of the radar signal and the interpretation of imagery. A series of radar reflectors were set out on the airfield to ground truth the digital program. By calculating the radar cross-section of each of these reflectors and with knowledge of their physical location an amplitude calibration can be carried out on the digital returns. Visual observations, snow pits and meteorological information collected at this site are essential for the Goose Bay image interpretation. This information is documented in this Field Data Report to make it available to researchers who will be working with the Goose Bay Data.

Centre for Cold Ocean Resources Engineering (C-CORE). Project SAR ’77 Summary Report. C-CORE Publication 79-15.

Radar images for Project SAR '77 were obtained during February and March of 1977. The data for sea ice is presented in this report. Data for other areas such as snow fields in New Brunswick and agricultural sites in Ontario will be reported elsewhere.

This report contains an analysis and the correlation of surface verification data at three field sites: Hopedale, Labrador; Twillingate, Newfoundland and the Ship-in-the-Ice Program. Data were also examined over Lake Melville and Groswater Bay. The analysis was carried out on survey processed data at C-CORE. Digital data were recorded for other researchers but was not part of C-CORE's mandate for this program.

Results are presented with specific examples. Reasons for the radar return from these examples are analyzed and discussed. Because the data were only surveyed processed recommendations are made on the further utilization of this data set.

Cormorant Ltd. (1997). 1997 Voisey’s Bay Ice Monitoring Program: Program Report. Prepared for Voisey’s Bay Nickel Company Limited, St. John’s, Newfoundland. December 11, 1997.

The overall intent of the 1997n Voisey’s Bay Ice Monitoring Program was to increase the knowledge base of the local ice conditions in the vicinity of the Voisey’s Bay mine and mill development. A better understanding of ice conditions will be important as VBNC considers social, environmental, and engineering implications of winter shipping in the area. The goal of this project was to develop a comprehensive picture of the ice conditions for a single season. The scope included the measurement of landfast ice extent and characteristics; measurement of atmospheric and ocean climate conditions during the ice season; and a description of pack ice conditions in the offshore approaches to the area. All field workers participating in this program were asked to note wildlife observations and human activities in the area. The focus of activities was the Potential Shipping Route (PSR) an area determined as the deepest water along the coastal channel with deep water vessels would navigate to reach the proposed VBNC marine terminal at Edward’s Cove.

Cormorant Ltd. (1998). 1998 Voisey’s Bay Ice Monitoring Program: Component Project Data Report 1. Landfast Ice Thickness Measurements Along the Voisey’s Bay Potential Shipping Route. Prepared for Voisey’s Bay Nickel Company Limited, St. John’s, Newfoundland. 3 August 1998.

This report presents landfast ice data collected along the inner portion of the Potential Shipping Route (PSR) leading to the proposed VBNC port facility at Edwards Cover in Anaktalak Bay. The report concentrates on physical landfast ice measurements conducted during the 1998 ice season,

including ice thickness, snow depth, and snow surface roughness. In addition, 1998 ice conditions along the PSR are compared to 1997 conditions.

Danielson, E.W (1971). Hudson Bay Ice Conditions. Arctic, Vol. 27 (2), pp. 90-106.

Monthly mean ice cover distributions for Hudson Bay have been derived, based upon an analysis of nine years of aerial reconnaissance and other data. Information is presented in map form, along with discussion of significant features. Ice break up is seen to work southward from the western, northern and eastern edges of the Bay; the pattern seems to be a result of local topography, currents, and persistent winds. Final melting occurs in August. Freeze-up commences in October, along the northwestern shore, and proceeds southward. The entire Bay is ice covered by early January, except for persistent shore leads.

DF Dickens Associates Ltd. (1997). Review of Historical Ice Conditions Affecting the Voisey's Bay Development. Prepared for Voisey's Bay Nickel Company Limited, St. John's, Newfoundland. September 30, 1997.

This project evaluates ice conditions along the proposed northern shipping route for Voisey's Bay Mine/Mill starting at the offshore approaches to Nain in the vicinity of 60° West Longitude, and ending at the approaches to Edward's Cove. Associated with the report is a database of ice concentrations spanning a 24-year time period from 1972 to 1996, and a collection of satellite images.

Ice first appears along the Labrador Coast in the vicinity of Nain between the beginning and end of December. There is considerable variability from year to year, with cases of first complete ice cover at Nain as early as late November and as late as mid-January. The ice which first forms in protected bays and channels, extends rapidly seaward to incorporate the offshore islands on the marine approaches to the Nain area (Dog Island, Sandy Island, Humbys Island, Spracklins Island).

The winter extent of the fast ice zone is highly variable from year to year, with the seaward edge ranging from the vicinity of Whale Island in January to the Hen and Chickens by April. Easterly edge locations are vulnerable to fracturing during onshore ice pressure events followed by subsequent break-away under strong offshore winds.

Hindcast estimates were made of fast ice thickness between 1984 and 1996, using a simple empirical growth model calibrated against both Hopedale records and 1997 field data. A realistic range in average April ice thickness along the proposed shipping route is considered to be between 110 and 140 cm, with peak values at some locations exceeding 150 cm. Unusually warm winters with heavy snow cover could result in a maximum thickness as low as 80 to 90 cm.

Pack ice on the approaches to the Nain area can vary in east-west extent from as little as 30 km to as much as 180 km (using 6/10 concentration as the seaward boundary). Rapid contractions and expansions of the pack ice are common, with the pack ice width often varying by as much as 80 km over a one-week period. High concentrations of pack ice routinely persist on the offshore approaches throughout the month of July, but similar conditions are more unusual inshore of Paul Island (five of the past 24 years).

Pack ice characteristics are extremely complex and at any given time, ice in this zone comprises a mix of locally grown new and young ice, together with thicker first-year floes and a small number of multi-year floes, moving constantly with the currents from north to south. Very large daily movements are common. One set of measurements in December and February (1977) recorded peak ice speeds as high as 120 km over 24 hours, with 10 percent of the readings exceeding 80 km. Two ice beacons deployed off Nain in January 1988 showed what appears to be a characteristic velocity shear between 60° and 58° Longitude moving offshore. The inshore beacon over the shelf (Nain Bank) moved at only one-third of the speeds recorded for the beacon over the slope (20 versus 58 cm/sec over 10 days).

Large areas of the pack are heavily deformed with surface features exceeding 3 m. First-year floe thickness is highly variable with maximum "level" values in the 1.8 to 2.2 m range by late April.

Multi-year ice is often present as small floes and fragments buried in the pack. Concentrations of this old ice rarely exceed 1/10. The thickness of multi-year floes is highly variable, depending on the degree of hummocking; mean values ranging from 2.8 to 6.7 m have been reported from field studies and stereo-photography.

Ice pressure can play an important role in vessel design, performance and scheduling. The potential for ice pressure was evaluated by examining discrete events with strong, sustained onshore winds exceeding 37 km per hour (20 knots) for a minimum of 8 hours. Nineteen such events were identified at times when there was a substantial amount of ice in the offshore area (over 6/10 of ice thicker than 30 cm). Durations of each event ranged from 9 to 33 hours, with average speeds ranging from 37 to 60 km per hour. The timing of events varied greatly from year to year but tended to concentrate in the months of March and April. An "average" year saw one potential ice pressure event lasting for 18 hours. The 1988 ice season stands out with six potentially serious ice pressure situations between March and June lasting a total of 109 hours.

DF Dickens Associates Ltd. (1997). Voisey's Bay 1996 Environmental Baseline Technical Data Report: Spring Ice Break-Up Survey. Prepared for Voisey's Bay Nickel Company Limited, St. John's, Newfoundland. October 30, 1997.

The 1996 spring ice breakup study was initiated to document the timing and progress of deterioration and clearing of the landfast ice within the geographic area being considered for potential shipping route. A secondary objective was to follow the final clearing of the pack ice from the area following landfast breakup. The results of this initial breakup survey is being compared with previous years in an ongoing study of the ice conditions in the Voisey's Bay area.

Environment Canada (1974). Ice summary and analysis 1971 Hudson Bay and approaches. 43 p. Canada

Break-up and disintegration of the ice was earlier than normal in northern Hudson Bay and in eastern Hudson Strait. In western Hudson Strait conditions were slightly later than normal while in southern Hudson Bay final clearing after mid September was the latest on record. Clearing of the Labrador coast and the approaches to Hudson Strait occurred early. An attempt is made to relate the pattern of ice disintegration and drift to the meteorological and oceanographic parameters affecting the area during the spring and summer period, and to indicate the patterns of freeze-up during the autumn months.

FENCO (1977). 1977 Winter Field Ice Survey Offshore Labrador. Prepared for TOTAL Eastcan Exploration Ltd, Calgary, Alberta. 30 August 1977. (confidential)

This report documents the measurements made during the winter program offshore Labrador. We conducted the following tests and observations. Ice thickness obtained from drilling holes and results of aerial photography. In situ ice strength tests to determine unconfined and confined compressive strengths and the elastic modulus. Ice salinity profiles. Ice temperature profiles. Surface topography measurements by means of aerial photographs. Aerial observations of ice conditions, both visually and by means of photography.

Freeman, N.G., J.C. Roff, and R.J. Pett (1982). Physical, chemical and biological features of river plumes under an ice cover in James and Hudson's Bays. Nat. Can. Que., 109, 745-764.

Observations of salinity, temperature, currents, nutrients and seston taken in February and March 1980 from the close-packed to solid ice cover off the La Grande River mouth provide a fairly detailed description of the flow and mixing of the river plume with the more saline basin water and the resulting effect on bio-chemical distributions. Within the first 5-10 km off the river mouth, a large horizontal divergence of the river flow, accompanied by a substantial reduction in average flow velocities in the plume, is observed. A significant thinning of the interface occurs in this region due to internal hydraulic control, but there is no apparent increase in entrainment of salt water into the

plume. For the next 25-30 km the interfacial Froude number is negative and the upper layer continues to thin out, indicating that surface water, with an estimated residence time of only 12 days, is being mixed downward due to increasing tidal action just under the plume. A frontlike feature, delineated by maximum horizontal gradients in density, separates this region from the well-mixed area beyond. In this latter region, shoaling bathymetry increases the tidal currents and vertical mixing of the water column seems to take place.

The biochemical distributions support the view of an earlier study that the La Grande River provides minimal nutrient contributions to James Bay in the winter. Nutrient values tend to be low within the plume and high within the basin, while the opposite is true of seston levels, thus suggesting marine and riverine sources, respectively. Under-ice concentrations of dissolved labile nutrients are largest in the well-mixed region seaward of the stabilizing surface plume and an ice flora community is well established in this area by the end of February. Levels of $N0_3 + N0_2$ in the surface ice and in the snow cover are generally a factor of two or three greater than those in the water immediately below the ice, indicating that melting ice and snow cover may be an important nutrient source to James and Hudson Bays during the spring phytoplankton bloom.

A comparison of the above physical data with salinity and current data collected off La Grande under the lower discharge conditions of 1976 and off Great Whale River (1979) where both discharge and background tidal conditions were substantially less, shows that the volume of freshwater in the plume is directly related to river discharge and inversely related to tidal kinetic energy in the basin. A correlation of estuarine Richardson number with top-to-bottom salinity difference also shows two distinct mixing regions: for Ri_E > 1-0 a stable region exists where mixing has a -1/6 power dependence on estuarine Richardson number and for Ri_E < 1.0 a well-mixed region, which has the typical -3/4 power dependence. In the initial region just off the river mouth, no significant entrainment or mixing into the plume is observed and thus no correlation of plume salinity with densimetric Froude number is obtained.

Godin, G. (1986). Modification by an ice cover of the tide in James Bay and Hudson Bay. Arctic, Vol. 39, pp. 65-67

The tide in Hudson Bay-James Bay is mainly semidiurnal. Admittance calculations between a reference signal and the water level observed at some gauging sites reveal that in the interior of Hudson Bay-James Bay the tide occurs earlier and its amplitude is reduced after the formation of an ice cover.

Gow, A.J. (1987). Crystal structure and salinity of sea ice in Hebron Fiord and vicinity, Labrador. U.S. Army Cold Regions Research and Engineering Laboratory, Hanover, New Hampshire. March 1987.

In this report we present results of measurements of the crystalline structure and salinity characteristics of sea ice in Hebron Fiord and vicinity, Labrador. Structurally, the fiord ice was entirely first-year and composed predominantly of congelation, columnar-type crystals. At most of the sampling sites the ice exhibited moderately to strong aligned c-axes consistent with the inferred direction of near-surface currents in the fiord. Generally diminished values of bulk salinity at five separate locations reflect the warm ice conditions encountered at the time of sampling (late May) and the effect of the meltwater flushing in promoting loss of brine, vertically, from the ice sheet. Observations outside Hebron Fiord indicated the presence of only minor amounts of multiyear ice during the latter part of May.

Ingram, R.G. and P. Larouche (1987). Variability of an under-ice river plume. J. Geophys. Res. 92: 9541-9547.

Observations of the Great Whale River plume in the coastal waters of Hudson Bay, Canada during late winter and early spring during four different years showed its area to vary as a power of the discharge. The under-ice plume area was much larger than plume area in open water for comparable

discharges. Differences in plume geometry were related to elapsed time since ice formation and low-frequency variability of the coastal circulation. The strength and orientation of the coastal motion was weakly correlated with the cross-Hudson Bay atmospheric pressure gradient. The passage of low pressure systems over Hudson Bay is thought to generate a progressive edge wave in the absence of direct wind forcing. The amplitude of the low frequency variations in coastal circulation decreased with the increasing special extent of the landfast ice in the study area.

Langleben, M.P (1959). Some Physical Properties of Sea Ice II. Can. J. Phys. Vol. 37.

Some properties of sea ice at mid-temperature latitudes are investigated. It is found that the salinity is comparable to, and the density much lower than, annual arctic sea ice. Permeability to air flow compares favourably to calculations based on the model of sea ice of Anderson and Weeks (1958). Small sample ring tests of ultimate tensile strength yield values ranging from 9.5 to 24.8 kg cm^{-2} at test temperatures of –3.6°C to –17.2°C. Tensile strength appears to depend on crystal size rather than on brine content.

Langleben, M.P. (1972). Decay of an annual cover of sea ice. Journal of Glaciology, 11(63), pp.337-344. United Kingdom.

In his now classic book *L'dy Arkliki (Arctic ice),* Zubov discussed the melting of sea ice during the Arctic summer by thermal interaction with the surrounding water and derived an expression which indicates that the proportion of open water increases exponentially with time until total ice-free conditions result. His equation predicts that the time required for complete decay of the ice cover after initial break-up is greater than one month and more likely as long as two months for representative values of incident shortwave radiation and initial ice thickness upon break-up. It is unlikely that above-freezing temperatures persist for this length of time.

To explain the observed complete disintegration of the annual ice cover in many sheltered areas of the Arctic, a modified model of the thermal decay process has been introduced. This model takes into account the influence of radiation absorbed by the ice which was not included in the Zubov formulation. Considerable reduction in the time required for complete decay, generally by about a factor of 2 if an albedo of 0.4 is assumed for the ice surface, is obtained.

Larnder, M.M. (1968). The ice. in Science, History and Hudson Bay, Vol.1, edited by C.S. Beals, pp. 318-341. Dept of Energy, Mines and Resources, Ottawa.

The contrast between the arctic and subarctic climate of Hudson Bay and the areas of comparable latitude in Europe is well illustrated by the difference in ice conditions along these two routes and the influence which they have on neighboring land areas. The North Sea and its connections with the Baltic are, for the most part, ice-free throughout the year, owing to heat transfer by winds and ocean currents from the Atlantic Ocean. The waters of the Hudson Bay, on the other hand, receive no ameliorating influences such as come to the waters of western Europe from the Gulf Stream and the relatively warm eastern Atlantic. The outstanding characteristic of the ice of Hudson Bay is its variability. Although a virtually complete ice cover spreads over the entire area each winter and disappears in the course of the following summer, the pattern of its formation and breakup differs widely from year to year and from one locality to another.

Larouche, P. and P.S. Galbraith (1989). Factors Affecting Fast-Ice Consolidation in Southeastern Hudson Bay, Canada. Atmosphere-Ocean, Vol. 27 (2), pp. 367-375. Canadian Meteorological and Oceanographic Society.

Analysis of satellite images of southeastern Hudson Bay taken over a period of 13 years led to the classification of ice distribution into three categories. The first category is for the complete fast ice-cover of the area, the second for fast ice covering only half the area and the third for the absence of fast ice extending away from the coast. Of the three factors considered- wind, water circulation and air temperature- the occurrence of strong southwesterly winds during the freezing period is probably

the main factor regulating the extent of the fast-ice cover for the first two categories. Through melting action, above-freezing air temperatures appear to prevent the consolidation of ice into a solid cover giving rise to the rare third category of ice distribution.

LeDrew, B.R., S.T. Culshaw. Ship-in-the-Ice Data Report. Centre for Cold Ocean Resources Engineering, St. John's, Canada. C-CORE Publication No. 77-28.

A small ice classed vessel, M/V "Arctic Explorer" was chartered for the month of February to provide a base for operations. Out of eighteen days in the study area, only six days were spent frozen in, ten days were spent moving or trying to move and two days were lost due to storm conditions. The report contains information on pack ice strain, ice and snow characteristics, photography and radiometric temperatures, water column measurements, and seabird/mammal counts.

Lepage, S. and R.G. Ingram (1991). Variation of Upper Layer Dynamics During Breakup of the Seasonal Ice Cover in Hudson Bay. Journal of Geophysical Research, Vol. 96, No. C7, pp. 12,711-12,724, July 15, 1991.

The present study describes circulation and stratification changes associated with the melt and breakup of the seasonal ice cover in the coastal waters of southeast Hudson Bay. Field work was carried out at a station located 25km north of the Great Whale River. Buoyancy fluxes and dissipation rates were calculated as well as changes in potential energy. Surface velocity data were partitioned into frequency bands and complex demodulated. Throughout the sampling period, most of the current energy was found to be in the semi-diurnal tidal band. After ice breakup, however, low frequency and inertial motions became relatively more important in response to direct wind forcing at the sea surface. Changes in amplitudes and phases of the major tidal constituents occurred and are related to the presence of the sea ice cover. Between early April and mid-June, semi-diurnal current amplitude doubled while its phase shifted by 45 to 60 degrees. In early June, the ice cover was sufficiently dispersed to allow the surface turbulence to overcome the buoyancy flux and mix the upper water columns.

Loset, S., A. Langeland, B. Bergheim & K.V. Hoyland (1998). Geometry and physical properties of a stamucha found on Spitsbergen. Proceedings of the 14th International Symposium on Ice (IAHR), Vol. 1, pp. 339-344. July 27-31, 1998.

A stamucha (grounded pressure ridge) was found in 'Van Mkienfiorden', Spitsbergen during February of 1997. The surface and keel geometry of the stamucha was surveyed between March and June, 1997. Temperature distribution was continuously monitored by thermistor strings, and drillings were made to estimate ridge porosity and composition. The stamucha measured 10x10 m at the water line and the maximum thickness was 4.4 m, with an average thickness of about 3.0 m. The estimated porosity ranged from 10 to 25 %. The paper presents the physical characteristics of the stamucha and relates the temperature data to consolidation and meteorological data from the area.

Martinson, C.R. Impulse radar sounding of level first-year sea ice from an icebreaker. U.S. Army Cold Regions Research and Engineering Laboratory, Hanover, New Hampshire. November 1985.

Location: Hebron Fjord. During the last weeks of May 1984, a CRREL impulse radar system was used onboard the RV Polarstern to measure the thickness of level first-year sea ice. The purpose was to determine the onboard performance of the radar system and, if possible, provide ice thickness information to researchers conducting other tests. Radar data were compared with ice thicknesses determined by drilling, indicating that radar sounding could be a viable means of collecting ice thickness information. A lack of adequate coordination between the two measurement methods prevented a point-by-point comparison of ice thickness. The comparisons were based on averages for particular test runs. The differences of the averages from the two measuring methods ranged form 0.03 m to 0.22 m with a mean variation in the differences of 0.13 m for eight runs. There may have been some interference from the ship's hull during data collection because of the location of the

antenna. However, an unidentified signal in some of the data does not appear to obscure a valid return from the bottom of the ice sheet.

McKenna, R. L. (1989). Section 8.7: Ice Mechanical Properties. LIMEX'89 Data Report. Energy, Mines and Resources Canada.

This project addresses the important phase during crushing in which distributed microcracks are formed, therefore reducing peak stresses. Ice in the Labrador margin is frequently near the melting point through its depths. These experiments represent an initial effort at characterizing the crack-enhanced creep properties of sea ice at a temperature of -2°C. Uniaxial compression tests were conducted at strain rates of $4x10^{-5}$ to $3x10^{-4}$ s^{-1}.were carried out on ice samples cut from the floes. The experiments were conducted in a portable cold room located on the deck of the MV Terra Nordica and finished in the laboratory facilities of the Faculty of Engineering and Applied Sciences at Memorial University.

Moore, B.D.H. and A.F. Gregory (1979). Monitoring and Mapping Sea-Ice Breakup and Freezeup of Arctic Canada from Satellite Imagery. Arctic and Alpine Research, Vol. 11(2), pp. 229-242.

The applications for NOAA and Landsat imagery for monitoring and mapping sea-ice breakup and freezeup are discussed. In particular, the results of studies using imagery collected over Canadian Arctic seas during July to November, 1975 through 1977, are presented in three maps. The maps indicate important features of areal and temporal variations in processes of sea-ice deformation and growth. This study has shown that much information concerning sea-ice breakup and freezeup can be obtained by combined use of NOAA and Landsat imagery. Moverover, it is suggested that satellite imagery could be used in obtaining long-term sea-ice statistical data which are necessary for climatological modeling and future planning of navigation as well as offshore gas and oil exploration in Arctic Canada.

Peterson, I.K. 1990. Sea ice velocity fields off Labrador and eastern Newfoundland derived from satellite imagery: 1984-1987. Can. Tech. Rep. Hydrogr. Ocean Sci. No. 129:vi + 85 pp.

A data set of 92 ice velocity fields off Labrador and eastern Newfoundland has been produced for the years 1984-1987 using pairs of sequential NOAA/AVHRR visible images, 1 day apart. The digital imagery was geometrically corrected using ephemeris data. The ice velocities are in good agreement with those obtained from satellite- tracked ice beacons. The velocity fields are useful in describing the spatial variability of ice velocity on scales of tens of kilometres or more, and reveal the importance of topographic steering of the currents.

Results from a regression analysis between ice velocity and geostrophic wind, using ice velocities derived from satellite imagery were similar to those using ice velocities derived from ice beacons. Over the Labrador/Newfoundland shelf south of 54.25°N under offshore wind conditions, ice moved at 1.8-2.0% of the geostrophic wind speed, with a negligible turning angle.

Pounder, E. R. and E. M. Little (1959). Some Physical Properties of Sea Ice I. Can. J. Phys. Vol. 37.

This preliminary study is based mostly on work done at a shore station in Shippegan, N.B. during the winter of 1956-57, with some data from an icebreaker expedition in the summer of 1956. The Shippegan site had unrafted ice, tides of 5 feet or less, and negligible fresh-water runoff. The thickness of the ice was about proportional to the square root of the freezing exposure. Tritium dating of sea ice is an unsatisfactory method because of variable tritium concentration in Arctic waters. The jaggedness of ice crystals is suggested as a measure combining effects of age and thermal regime. Measurements of specific gravity, salinity, electrical resistivity, and permeability profiles all show progressive changes in annual sea ice throughout the winter. The tensile strength of sea ice at –20°C was around 200 to 500 p.s.i., at various angles to the grain. For fresh water ice, with stress parallel to

the grain, it was in the range 500 to 1000 p.s.i. Shear strengths, with the shear plane parallel to the grain, were 80 to 160 p.s.i. for sea ice at –20°C and 160 to 280 p.s.i. for pond ice, also at –20°C.

Prinsenberg, S.J. (1980). Man-made changes in the freshwater input rates of Hudson and James Bays. Can. J. Fish. Aquat. Sci., Vol. 37, pp. 1101-1110.

The freshwater input rates of the Hudson/James Bay region were obtained on a monthly time scale and include contributions of evaporation, precipitation, and river runoff. The yearly mean precipitation minus evaporation rate shows that it behaves as an oceanic region supplying the overlying air mass with moisture. The monthly runoff rates for the total region and James Bay alone have minimum values during the winter and maximum values during the spring freshet. The total freshwater input can be divided into a winter and summer season. The large input of the summer represents an average monthly addition of a 10.0-cm layer of fresh water while the smaller winter input amounts to addition of a 0.5-cm layer of freshwater. Annually, the total surface area receives a layer of 64 cm of freshwater.

During the 1980s, four hydroelectric developments will cause temporal changes in the freshwater input cycle as winter river runoff rates will increase to values comparable to spring peak runoffs. in the Nelson-Churchill River development, the Churchill River runoff will be reduced to 29% of its natural state during the winter and to 54% during the summer. This water will increase the runoff into the Nelson River Delta by 52% in the winter and 10% in the summer. Similarly, the Eastmain River runoff will be reduced by 79%. The La Grande River will double its yearly averaged runoff rate and experience a 500% increase in runoff during the winter. The other two developments, Nottaway-Broadback-Rupert rivers (N.B.R.) and Great Whale-Little Whale proposals, will experience similar changes: large increases in the winter runoff rates and small decreases in summer rates.

The total freshwater input into James Bay will be doubled during the winter months. In addition, half the future input will occur in the northern region which now receives only 20%. The La Grande River winter runoff rate will equal in magnitude that of the Nelson River Delta which presently accounts for 25% of the Hudson/James Bay winter runoff. The runoff for the total Hudson/James Bay region will also experience the largest changes during the winter when the average monthly runoff rate will increase by 52%, due largely to the La Grande Complex. On the other hand, the summer runoff rate for the total region will decrease by 6%.

Prinsenberg, S.J. (1986) Man-made changes in the freshwater input rates of Hudson and James Bays. in Canadian Inland Seas by I.P. Martini, pp. 163-186.

Oceanographic data have been collected in Hudson Bay and James Bay during summer and winter when either research vessels or helicopter could be used. During the fall and spring the seasonal ice cover forms or decays which makes data collection extremely difficult. Most of the data for central Hudson Bay is from the summer with some winter data available from southeastern Hudson Bay and James Bay. A current meter mooring from 150 km northeast of Churchill collected the only year-round salinity and temperature data set of the region. All available data are used to determine the surface and subsurface circulation patterns and to what extent they are influenced by the seasonal cycles of the ice cover, runoff and radiation heat flux.

Prinsenberg, S.J. (1987). Seasonal Current Variations Observed in Western Hudson Bay. Journal of Geophysical Research, Vol. 92, No. C10, pp. 10756-10766, September 15, 1987.

Yearlong current meter data from western Hudson Bay show that the annual ice cover modifies the currents. Currents observed at three depths are dominated by barotropic semidiurnal tidal currents which reach amplitudes of 28 cm s^{-1}. During the ice-covered season the tidal currents and tidal heights observed inshore decrease, and their arrival times are advanced. Monthly mean currents set predominantly to the south and east in accordance with the cyclonic circulation pattern of the bay. Mean current speeds are less than 4 cm s^{-1} and are made up of wind-driven and density-driven

components. Their onshore-offshore components vary in phase with the ice buildup and ice breakup seasons of the annual ice cover. Storm-generated inertial currents are as strong as the tidal currents but rotate clockwise, opposite to the tidal current direction. They decrease with depth and are absent during the ice-covered season. Inertial currents below the pycnocline lead those in the surface mixed layer by more than 180°, simulating and upward phase velocity. Passing weather systems also generate 5- to 6- day periodic currents which slightly decrease but are coherent with depth. They reach magnitudes of up to 25 cm s^{-1} and occur throughout the year, regardless of the ice condition.

Prinsenberg, S.J. (1988). Ice-cover and ice-ridge contributions to the freshwater contents of Hudson Bay and Foxe Basin. Arctic, Vol. 41, pp. 6-11.

Runoff and Precipitation add 65cm of fresh water to Hudson Bay annually. The ice cover does not count for a net contribution of fresh water over a one-year period; however, on weekly time scales, it contributes as much or more than runoff. The maximum thickness of ice averaged over the Bay is 160cm and represents a 140cm layer of fresh water when sublimation is accounted for. This fresh water is twice as large as the amount annually brought in by runoff and precipitation and is added to the surface layer in the spring and removed from the surface layer in the fall.

Freshwater budgets of Hudson Bay and Foxe Basin indicate up to 90% more ice is produced than indicated by ice thickness data. Part of this difference can be attributed to the ice accumulated in ice ridges, which for Hudson Bay accounts for 25cm of ice and as much as 58cm ice for Foxe Basin, where extreme rough ice conditions occur.

Prinsenberg, S.J. and I.K. Peterson (1992). Sea-Ice Properties off Labrador and Newfoundland During LIMEX '89. Atmosphere-Ocean, Vol. 30 (2), pp. 207-222. Canadian Meteorological and Oceanographic Society. June 1992. Canada

During the cold winter of 1988/89, ice coverage was abnormally high over the Newfoundland Shelf, but was low over the northern Labrador Shelf. The pack-ice aligned in bands parallel to the coast and bathymetry, with thin ice and open water occurring inshore of the thick pack-ice, a result of ice divergence along the coast and the large ice melt rates at the shelf break. Freezing degree-day models predicted higher than normal ice thicknesses at land-fast ice stations when climatic mean snow-layer depths were used. However, observed ice thicknesses were below normal, which could only be predicted when observed snow conditions were used. Offshore winds generated ice divergence, which stimulated increased ice growth in the nearshore region, which in turn caused the large surface mixed layer depths and high salinity values. Ice drift rates obtained from satellite-tracked ice beacons had two-week averaged speeds of 18 km/day, equal to the large horizontal melt rates of the ice edge over the shelf break bordering the Labrador Sea. Ice drift rates up to 75 km d^{-1} were observed during strong northwesterly winds over the continental slope where the Labrador Current is located.

Raney, R.K., S. Digby Argus and L. NcNutt (1989). Labrador Ice Margin Experiment LIMEX'89; An Overview. IGARSS Int. Geosci. and Remote Sensing Symp.Vol. 3 Part 3, Page 1517-1519.

LIMEX (Labrador Ice Margin Experiment) was conceived as a series of multidisciplinary experiments, to prepare for the optimal use of microwave data from the satellites ERS-1, J-ERS-1, RADARSAT and SSM\I. The primary objective of LIMEX'89 was to establish a link between the status and evolution of ice and ocean properties in the economically important Labrador marginal ice zone (MIZ) and corresponding remotely sensed data, particularly Synthetic Aperture Radar (SAR) imagery. LIMEX'89 took place off the East coast of Newfoundland, 4 March -4 April. The international and multifacility experiment was highly successful and met or exceeded LIMFX data objectives and the data requirements of most investigators. Initial indications are that the data will produce exciting results and substantially enhance understanding of microwave response to ice and ocean conditions and processes typical of the Southern Labrador Sea.

Rescan Environmental Services Limited (1997). Physical Oceanography of the Voisey's Bay Project Area- Voisey's Bay Nickel Company Environmental Impact Assessment. Prepared for Voisey's Bay Nickel Company Limited, St. John's, Newfoundland. November 1997.

Current meters and tide gauges collected data in Anaktalak, Kangeklualuk and Voisey's Bays from July, 1995 through October, 1996. In addition, conductivity, temperature and depth profiles were measured throughout the area.

Year-long current, temperature and salinity data reveal a picture of strong stratification forming at break-up, continuing through freshet in July and then progressively weakening through October. Vertically homogenous conditions are present in November. From January to May the entire water column is at or very near its freezing point at all locations.

Currents are weak, generally less than 10 cm/s, except in the passage between Anaktalak and Voisey's Bays where tidal currents probably exceed 100 cm/s locally. These energetic currents break down vertical density stratification by August.

Tides are strongly semi-diurnal with spring ranges up to 2.5 m.

Steel, A., J.I. Clark and P. Morin (1994). A comparison of pressuremeter test results in sea ice. Canadian Geotechnical Journal, Vol. 31, No. 2, pp. 254-260.

The results of short-term pressuremeter tests from three different sea ice environments are presented. These results are used to derive mechanical properties of the ice, to compare the ice types, and to evaluate the Texam pressuremeter as an instrument for the field assessment of ice sheets and ice packs. The results are also compared with those existing in the literature. It was found that the strength of the sea ice was affected most significantly by temperature, but also by salinity and to a lesser extent by confining pressure and ice structure. The Texam pressuremeter operated well in the given field environment and will prove to be a valuable piece of equipment for determining the characteristics of these important ice formations.

Tan, F.C. and P.M. Strain (1996). Sea ice and oxygen isotopes in Foxe Basin, Hudson Bay and Hudson Strait, Canada. Journal of Geophysical Research, Vol. 101 (C9), pp. 20869-20876. September 15, 1996. United States.

The summer distribution of sea ice meltwater and river runoff and the surface circulation in Foxe Basin, Hudson Bay and Hudson Strait have been studied by oxygen isotope techniques. On the basis of oxygen isotope and salinity relationships, the reduction of surface salinity in summer in Foxe Basin is predominantly due to sea ice meltwater. River runoff and sea ice meltwater contribute equally to the summer surface layer in northern Hudson Bay. The isotopic data clearly show the flow of Foxe Basin water through Roes Welcome Sound into northwestern Hudson Bay, but no evidence for this outflow is found in the passages connecting Hudson Bay and Hudson Strait. Oxygen isotopes indicate that recent river runoff is concentrated in a narrow band along the south side of Hudson Strait. The wide variety of relationships between oxygen isotope ratios and salinity is explained by the known ice dynamics and the seasonal variability predicted from ice melting and freezing models.

Transportation Development Centre (1985). Trials off the Labrador Coast May 1984, Transport Canada. Edited by: R. Frederking and J.E. Laframboise. Polarstern: Report from the Canadian Team. May 1985.

In May 1984, the Federal German Republic F.S. Polarstern, an oceanic research vessel, was taken to the Labrador coast for the trials covering its icebreaking and ice transiting capabilities. The Hamburgishe Schiffbau Versuchsanstalt (HSVA) was responsible for the scientific content of these trials. A number of tests were carried out covering performance of the ship's systems in ice, ice breaking resistance in level ice and in ridges and structural response to ice loads. Trials took place off the coast of Labrador, in the Nain to Saglek region, and within the Hebron Fjord. Level ice with a thickness of 1 m was encountered, with some surface water and ramming attempted on ridges with keels exceeding 12 m in depth. Report summarizes observations of the members of the Canadian

team aboard the ship, comments by Coast Guard Pollution Control officers and report by the Labrador Inuit Association representatives on effect of the ship's passage through seal breeding areas.

Veitch, B, P. Kujala, P. Kosloff and M. Lepparanta. Field Measurements of the Thermodynamics of an Ice Ridge. Helsinki University of Technology, Faculty of Mechanical Engineering, Laboratory of Naval Architecture and Marine Engineering. 1991

A field programme dealing with the thermodynamic characteristics of ice pressure ridges in the Baltic Sea was carried out in the winter of 1990-91. The data collected during the field work are presented and some general observations are made. The measurements consisted of cross-sectional drilling and long-term temperature recording of an ice pressure ridge in the northern Bay of Bothnia. Drilling and temperature measurement results indicated that significant changes occurred in the ridge, including ridge sinkage, melting of the keel bottom, an increase in the thickness of the consolidated zone, and a decrease in porosity. The measured thickness of the ice comprising the ridge consolidated zone was found to be well predicted by a modified Stefan's equation for level ice growth. The thickness of the consolidated zone increased about 1.3 times as much as the level ice under the same ambient conditions.

Wang, J., L.A. Mysak and R.G. Ingram (1994). Interannual Variability of Sea-Ice Cover in Hudson Bay, Baffin Bay and Labrador Sea. Atmosphere Ocean, Vol. 32 (2) 1994, pp. 421-447. Canadian Meteorological and Oceanographic Society.

The spatial and temporal relationships between subarctic Canadian sea-ice cover and atmospheric forcing are investigated by analysing sea-ice concentration, sea level pressure and surface air temperature data from 1953 to 1988. The sea-ice anomalies in Hudson Bay, Baffin Bay and the Labrador Sea are found to be related to the North Atlantic Oscillation, (NAO) and the Southern Oscillation (SO). Through a spatial Student's t-test and a Monte Carlo simulation, it is found that sea-ice cover in both Hudson Bay and the Baffin Bay-Labrador Sea region responds to a Low/Wet episode of the SO (defined as the period when the SO index becomes negative) mainly in summer. In this case, the sea-ice cover has a large positive anomaly that starts in summer and continues through to autumn. The ice anomaly is attributed to the negative anomalies in the regional surface air temperature record during the summer and autumn when the Low/Wet episode is developing. During strong winter westerly wind events of the NAO, the Baffin Bay-Labrador Sea ice cover in winter and spring has a positive anomaly due to the associated negative anomaly in surface air temperature. During the years in which strong westerly NAO and Low/Wet SO events occur simultaneously (as in 1972/73 and 1982/83), the sea ice is found to have large positive anomalies in the study region; in particular, such anomalies occurred for a major portion of one of the two years. A spectral analysis shows that sea-ice fluctuations in the Baffin Bay-Labrador Sea region respond to the SO and surface air temperature at about 1.7, 5 and 10-year periods. In addition, a noticeable sea-ice change was found (i.e. more polynyas occurred) around the time of the so-called "climate jump" during the early 1960s. Data on ice thickness and on ice-melt dates from Hudson Bay are also used to verify some of the above findings.

Weeks, W.F. and O.S. Lee (1958). Observations on the Physical Properties of Sea-Ice at Hopedale, Labrador. Arctic, Vol. 11(3), pp. 135-155. September 1958. Canada.

During the last three winters the Air Force Cambridge Research Center, the Navy Hydrographic Office and the Snow, Ice and Permafrost Research Establishment have sponsored a joint project to study the general physical properties of sea ice by direct observation in the field. This paper reports some preliminary results obtained from data collected during the winter of 1955 to 1956 at Hopedale, Labrador.

Winsor, W.D., G.B. Crocker, R.F. McKenna, and C.L. Tang (1990). Sea Ice Observations during LIMEX, March - April 1989. Canadian Data Report of Hydrography and Ocean Sciences No. 81: iv, 43 pp.

Data of sea ice properties collected on *M/V Terra Nordica* during LIMEX'89 (Labrador Ice Margin Experiment) are documented. The data include ice thickness, ice drift, ice temperature and salinity, ice strength, and floe size distribution. Statistics and geographic distribution of these parameters are displayed.

Appendix B: Ice Thickness Polynomial Expressions

Ice Thickness Polynomial Expressions as a Function of Julian Day (JD)

Chesterfield Inlet:
h_i = 2.485723596E-11*(JD)^5 - 5.056418804375E-08*(JD)^4 + 0.000040901412954444*(JD)^3 - 0.0164099783565433*(JD)^2 + 3.24877261032555*(JD) - 252.955318805145

Churchill
h_i = 1.121108682E-11*(JD)^5 - 2.491030403439E-08*(JD)^4 + 0.0000221593339367353*(JD)^3 - 0.0098001045533722 9*(JD)^2 + 2.13545289701352*(JD) - 182.721086727511

Moosonee
h_i = 7.572163244E-11*(JD)^5 - 1.5121102291985E-07*(JD)^4 + 0.00012049403939461 2*(JD)^3 - 0.047864140419755*(JD)^2 + 9.46652130154259*(JD) - 745.003657776615

Hopedale
h_i = 2.009842626E-11*(JD)^5 - 4.101332495717E-08*(JD)^4 + 0.0000336319933752226*(JD)^3 - 0.0138150485484072*(JD)^2 + 2.82744995677231*(JD) - 229.593880606488

Resolute
h_i = 0.00000000000691*(JD)^5 - 0.00000001354392*(JD)^4 + 0.00001054502673*(JD)^3 - 0.0040624088985*(JD)^2 + 0.76314114385189*(JD) - 55.5634755891013

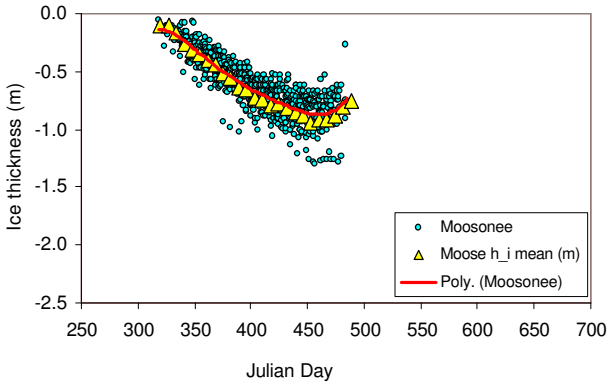

(a) Moosonee

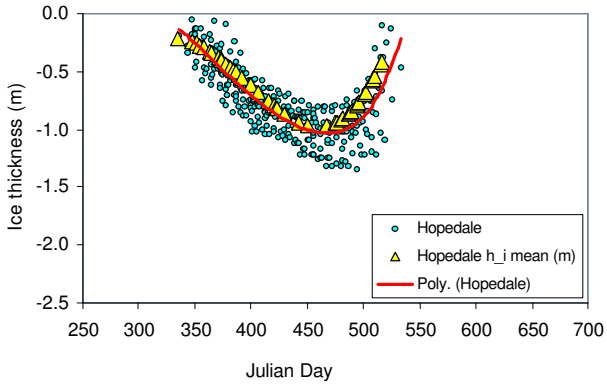

(b) Hopedale

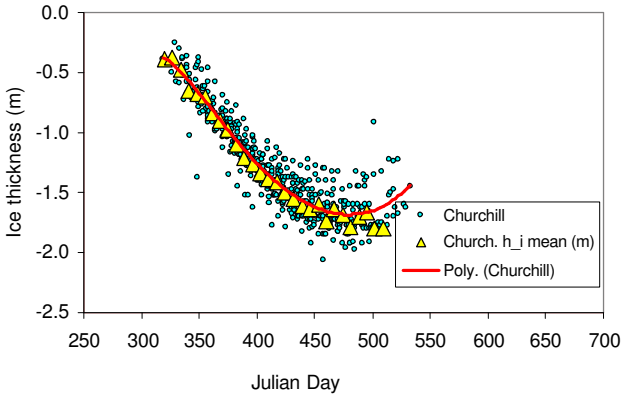

(c) Churchill

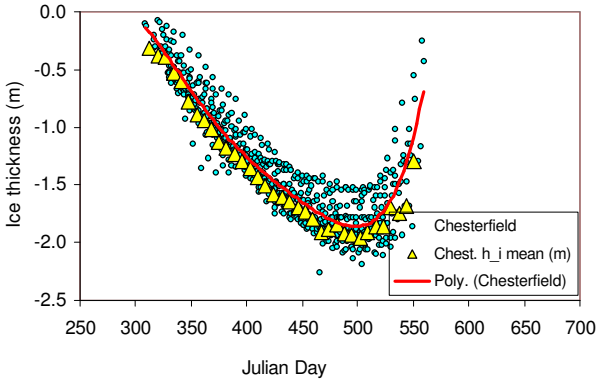

(d) Chesterfield Inlet

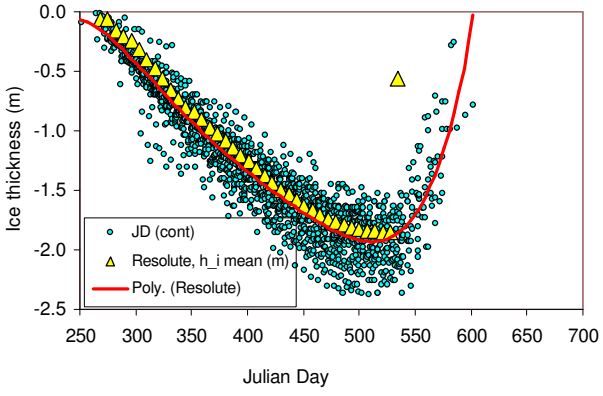

(b) Resolute

Figure B-1 Comparison of ice thickness data for selected sites